Flocking for Multi-Agent Dynamic Systems: Algorithms and Theory

Reza Olfati-Saber, *Member, IEEE*

***Abstract*—In this paper, we present a theoretical framework for design and analysis of distributed flocking algorithms. Two cases of flocking in free-space and presence of multiple obstacles are considered. We present three flocking algorithms: two for free-flocking and one for constrained flocking. A comprehensive analysis of the first two algorithms is provided. We demonstrate the first algorithm embodies all three rules of Reynolds. This is a formal approach to extraction of interaction rules that lead to the emergence of collective behavior. We show that the first algorithm generically leads to regular fragmentation, whereas the second and third algorithms both lead to flocking. A systematic method is provided for construction of cost functions (or collective potentials) for flocking. These collective potentials penalize deviation from a class of lattice-shape objects called α-lattices. We use a multi-species framework for construction of collective potentials that consist of flock-members, or α-agents, and virtual agents associated with α-agents called β- and γ-agents. We show that migration of flocks can be performed using a peer-to-peer network of agents, i.e., "flocks need no leaders." A "universal" definition of flocking for particle systems with similarities to Lyapunov stability is given. Several simulation results are provided that demonstrate performing 2-D and 3-D flocking, split/rejoin maneuver, and squeezing maneuver for hundreds of agents using the proposed algorithms.**

***Index Terms*—Consensus theory, distributed control, dynamic graphs, mobile sensor networks, networked autonomous vehicles, self-assembly of networks, self-organizing systems, swarms.**

I. Introduction

FLOCKING is a form of collective behavior of large number of interacting agents with a common group objective. For many decades, scientists from rather diverse disciplines including animal behavior, physics, biophysics, social sciences, and computer science have been fascinated by the emergence of flocking, swarming, and schooling in groups of *agents* with local interactions [1]–[12]. Examples of these agents include birds, fish, penguins, ants, bees, and crowds. In an abstract fashion, we refer to the members of flocks as α-*agents*.

The engineering applications of flocking include massive distributed sensing using mobile sensor networks in an environment; self-assembly of connected mobile networks; automated parallel delivery of payloads; and performing military missions such as reconnaissance, surveillance, and combat using cooperative unmanned aerial vehicles (UAVs). In nature, flocks are examples of self-organized networks of mobile agents capable of coordinated group behavior. The self-organizing feature of flocks/schools [12] can provide a deeper insight in design of *sensor networks* [13]–[16].

In 1986, Reynolds introduced three heuristic rules that led to creation of the first computer animation of flocking [5]. Here, are the three flocking rules of Reynolds

1) Flock Centering: attempt to stay close to nearby flockmates;
2) Collision Avoidance: avoid collisions with nearby flockmates;
3) Velocity Matching: attempt to match velocity with nearby flockmates.

Let us mention that these rules are also known as *cohesion*, *separation*, and *alignment* rules in the literature. These rules are subject to broad interpretation that complicates objective analysis and implementation of Reynolds rules.

Among the first groups of physicists who studied flocking from a theoretical perspective were Vicsek *et al.* [6], Toner and Tu [7], Shimoyama *et al.* [8], and Levine *et al.* [17]. The work of Vicsek *et al.* was mainly focused on emergence of alignment (which does not amount to flocking) in self-driven particle systems, whereas Toner and Tu used a continuum mechanics approach. Levine *et al.* created rotating swarms known as circular *ant mills* using a particle-based model with all-to-all interactions. Other continuum models of swarms were proposed by Mogilner and Eldstein-Keshet [18], [9] and Topaz and Bertozzi [19]. Helbing *et al.* [10] studied the *escape panic phenomenon* using an empirical particle-based model of flocks.

Recently, there has been a surge of interest among control scientists in *consensus problems* due to the work of Olfati-Saber and Murray [20], [21] and *alignment* on networks with variable topology by Jadbabaie *et al.* [22], Moreau [23], and Ren and Beard [24]. In alignment, there is no constraint on the consensus value, whereas in most consensus problems for networked dynamic systems, the objective is distributed computation of a function via agreement [20], [25].

Stability analysis of small groups of particles or agents with all-to-all interconnections were considered in [26]–[28]. Tanner *et al.* in [29] proposed a centralized algorithm for a particle system that leads to *irregular collapse* for generic initial states. They also suggest a distributed algorithm that leads to *irregular fragmentation*. Fragmentation and collapse are two well-known pitfalls of flocking that are discussed later.

Some past research with strong connections to this paper include the work of Fax and Murray [30] on formation control and graph Laplacians; Mesbahi [31], [32] on state-dependent

Manuscript received June 25, 2004; revised August 10, 2005 and November 21, 2005. Recommended by Associate Editor E. Jonckheere. This work was supported in part by the Air Force Office of Scientific Research under Grant F49620-01-1-0361 and in part by the Defense Advanced Research Projects Agency under Grant F33615-98-C-3613.

The author is with the Thayer School of Engineering, Dartmouth College, Hanover, NH 03755 USA (e-mail: olfati@dartmouth.edu).

Digital Object Identifier 10.1109/TAC.2005.864190

graphs; Cortes and Bullo [15] and Cortes *et al.* [33] on placement of mobile sensors; Rabichini and Frazzoli [34] on energy-efficient splitting algorithms; Leonard and Fiorelli [35] and Olfati-Saber and Murray [36] on graph-induced potential functions for structural formation control; Ögren *et al.* [37] on coordination of mobile sensor networks; Khatib [38] and Rimon and Koditschek [39] on using artificial potentials for obstacle avoidance; Strogatz [40] on complex biological and social networks; and Olfati-Saber [41] on ultrafast small-world networks.

A number of recent papers on motion control for swarms suffer from common drawbacks including the use of unbounded forces for collision avoidance, lack of scalability, and irregular fragmentation and collapse. In contrast, the work in [42]–[44] do not possess such features. In [43], some analytical results such as asymptotic alignment and energy dissipation are established. The analysis presented in [43] and some other existing works on flocking are far from complete. In particular, the existence of a spatial order in flocks has never been established. In this paper, we attempt to bridge some of these theoretical gaps by answering the following *fundamental questions*.

1) How do we design scalable flocking algorithms and guarantee their convergence?
2) What are the stability analysis problems related to flocking?
3) What types of order exist in flocks?
4) How do flocks perform split/rejoin maneuvers or pass through narrow spaces?
5) How do flocks migrate?
6) What constitutes flocking?

We hope that our analysis sheds light on cooperation and emergence of collective behavior in complex organizations.

Let us refer to a particle/agent in a group with the objective of performing flocking as an α-*agent*. We introduce three scalable flocking algorithms for α-agents. Our first algorithm is a gradient-based algorithm equipped with a velocity consensus protocol. We demonstrate that the first algorithm embodies all three rules of Reynolds. It is also demonstrated that this algorithm leads to regular fragmentation rather than flocking for generic initial states. The analysis of the first algorithm is very useful for clarifying the features of the regular fragmentation phenomenon. The second algorithm (or Algorithm 2) is the main flocking algorithm for moving in a free m-space. This algorithm has an additional term represented by a γ-agent that takes the group objective into account. In the process of analyzing Algorithm 2, we pose two conjectures that are crucial in explaining the spatial order of flocks and self-assembly of a connected network of mobile agents.

The third algorithm has obstacle avoidance capabilities. We represent the effects of obstacles via virtual agents called β-agents. These agents are kinematic and move on the boundary of the obstacles. A mutli-species collective potential is then formed that is used for both design and analysis of the third flocking algorithm. We demonstrate that the tracking problem for flocks can be solved using a peer-to-peer architecture without leaders—thus, confirming a widely accepted opinion by animal behavior scientists that "schools need no leaders" [1]. We provide several simulation results for 40—150 agents that successfully perform 2-D flocking, 3-D flocking, 2-D regular fragmentation, split/rejoin maneuver, and squeezing maneuver in a distributed manner.

The main contribution of this paper is to provide a theoretical and computational framework for design and analysis of scalable flocking algorithms in $\mathbb{R}^m$ in presence or lack of obstacles.

An outline of the paper is as follows: Some background on graphs, proximity nets, α-lattices, algebraic graph theory, consensus problems, collective potentials are presented in Section II. Two distributed flocking algorithms for moving in free-space are provided in Section III. Collective dynamics of flocks and a decomposition lemma are stated in Section IV. Our main results on analysis of the first two algorithms are presented in Section V. The relation between Algorithm 1 and Reynolds rules are established in Section VI. The third algorithm with obstacle avoidance capabilities is presented in Section VII. Extensive simulation results are provided in Section VIII. In Section IX, we elaborate on what constitutes flocking and give a universal definition of flocking. Finally, concluding remarks are made in Section X.

II. Preliminaries

The theoretical framework presented in this paper relies on some basic concepts in graph theory [45]–[47], algebraic graph theory [48], spatially induced graphs (or proximity nets) [43], and consensus problems [20], [21] that are discussed in the following.

A. Topology of Flocks: Proximity Nets

A *graph* G is a pair $(\mathcal{V},\mathcal{E})$ that consists of a set of vertices $\mathcal{V}=\{1,2\ldots,n\}$ and edges $\mathcal{E}\subseteq\{(i,j):i,j\in\mathcal{V},j\neq i\}$ (i.e., the graph is in general directed and has no self-loops). The graph G is said to be *undirected* if $(i,j)\in\mathcal{E}\iff(j,i)\in\mathcal{E}$. The quantities $|\mathcal{V}|$ and $|\mathcal{E}|$ are, respectively, called *order* and *size* of the graph. For networked dynamic systems, $|\mathcal{E}|$ is called *communication complexity* of the system [49].

The *adjacency matrix* $A=[a_{ij}]$ of a graph is a matrix with nonzero elements satisfying the property $a_{ij}\neq 0\iff(i,j)\in\mathcal{E}$. The graph is called weighted whenever the elements of its adjacency matrix are other than just 0-1 elements. Here, we mostly use weighted graphs with position-dependent adjacency elements. For an undirected graph G, the adjacency matrix A is symmetric (or $A^T=A$). The set of *neighbors* of node i is defined by

$$N_i=\{j\in\mathcal{V}:a_{ij}\neq 0\}=\{j\in\mathcal{V}:(i,j)\in\mathcal{E}\}. \tag{1}$$

Let $q_i\in\mathbb{R}^m$ denote the position of node i for all $i\in\mathcal{V}$. The vector $q=\mathrm{col}(q_1,\ldots,q_n)\in Q=\mathbb{R}^{mn}$ is called the *configuration* of all nodes of the graph. A *framework* (or *structure*) is a pair (G,q) that consists of a graph and the configuration of its nodes.

Consider a group of *dynamic agents* (or *particles*) with equation of motion

$$\begin{cases}\dot{q}_i=p_i\\ \dot{p}_i=u_i\end{cases} \tag{2}$$

where $q_i,p_i,u_i\in\mathbb{R}^m$ (e.g., $m=2,3$) and $i\in\mathcal{V}$. The benefit of using particle-based models of flocks compared to continuum

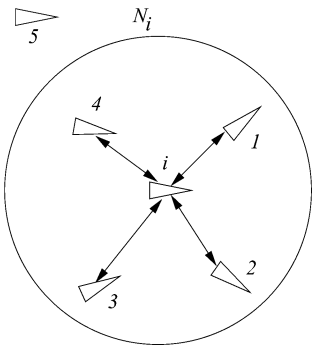

Fig. 1. Agent and its neighbors in a spherical neighborhood.

models is that one cannot take inter-agent sensing, communication, and computational issues for granted.

Let $r > 0$ denote the *interaction range* between two agents. An open ball with radius r (see Fig. 1) determines the set of *spatial neighbors* of agent i that is denoted by

$$N_i = \{j \in \mathcal{V} : \|q_j - q_i\| < r\} \tag{3}$$

where $\|\cdot\|$ is the Euclidean norm in $\mathbb{R}^m$. Given an interaction range $r > 0$, a *proximity net* $G(q) = (\mathcal{V}, \mathcal{E}(q))$ can be defined by $\mathcal{V}$ and the set of edges

$$\mathcal{E}(q) = \{(i,j) \in \mathcal{V} \times \mathcal{V} : \|q_j - q_i\| < r, i \neq j\} \tag{4}$$

that clearly depends on q. The framework $(G(q), q)$ is called a *proximity structure*.

The topology of a wireless sensor network with a radio range r is a proximity net [14]. If the interaction range of all agents is the same, the proximity net $G(q)$ becomes an undirected graph. The proximity net of n points is generically a digraph under either of the following assumptions: i) the spherical neighborhoods of agents do not have the same radius, or ii) every agent uses a conic neighborhood to determine its neighbors as in [5]. In this paper, all proximity nets are bidirectional graphs.

B. Geometry of Flocks: α-Lattices

To capture an apparent spatial-order in real-life flocks, we use a lattice-type structure to model the geometry of desired conformation of agents in a flock. For doing so, we seek the set of configurations q of n points in which each point is equally distanced from all of its neighbors on a proximity net $G(q)$. In terms of interagent distances, this geometric object can be described as solutions of the following set of algebraic constraints:

$$\|q_j - q_i\| = d \qquad \forall j \in N_i(q). \tag{5}$$

The solutions q of the set of constraints in (5) play the role of desired conformations of agents in a flock (i.e., a geometric model of flocks). Since, this geometric object frequently appears in this paper, we find it convenient to define it as a lattice-type object.

Definition 1 (α-Lattice): An *α-lattice* is a configuration q satisfying the set of constraints in (5). We refer to d and $\kappa = r/d$ as the *scale* and *ratio* of the lattice, respectively.

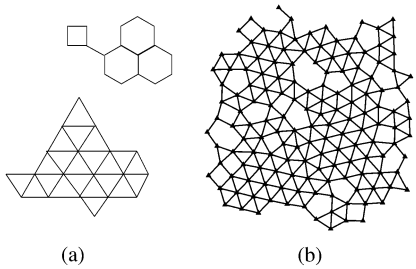

Fig. 2. Examples of α-lattices and quasi α-lattices: (a) a 2-D α-lattice with a disconnected proximity net and (b) a 2-D quasi α-lattice with $n = 150$ nodes.

The proximity net induced by an α-lattice is not required to be connected. Furthermore, all edges of the proximity structure induced by an α-lattice have the same length. Fig. 2 illustrates other examples of α-lattices.

Remark 1: As seen in Fig. 2, it turns out that the proximity structure of 2-D α-lattices are collections of *crystals (or quasicrystals)* that are made out of repeated use of a single (or multiple) type(s) of polygonal cells. This follows from planarity property of such proximity structures (see Theorem 4).

To describe conformations q' that are very close to an α-lattice satisfying (5), we use the following set of inequalities

$$-\delta \leq \|q_j - q_i\| - d \leq \delta \qquad \forall (i,j) \in \mathcal{E}(q) \tag{6}$$

and refer to its solutions as a *quasi α-lattice*. Fig. 2(b) illustrates a quasi-α-lattice that is computed numerically using the second flocking algorithm [or protocol (24)].

To measure the degree in which a configuration q differs from an α-lattice, we use the following *deviation energy*:

$$E(q) = \frac{1}{(|\mathcal{E}(q)| + 1)} \sum_{i=1}^{n} \sum_{j \in N_i} \psi(\|q_j - q_i\| - d) \tag{7}$$

where $\psi(z) = z^2$ is called a pairwise potential (note that other scalar potentials can be used as well). The deviation energy can be viewed as a nonsmooth potential function for a system of n particles. Interestingly, α-lattices are *global minima* of this potential function and achieve the minimum value of zero. For a quasi α-lattice q with an edge-length uncertainty of δ, the deviation energy is given by

$$E(q) \leq \frac{|\mathcal{E}(q)|}{|\mathcal{E}(q)| + 1} \delta^2 \leq \delta^2 = \varepsilon^2 d^2, \qquad \varepsilon \ll 1$$

which means *quasi α-lattices are low-energy conformations of n points*. The order of magnitude of the deviation energy of the quasi-α-lattice in Fig. 2(b) is 10^{-3} (for $d = 7$ and $\kappa = 1.2$).

C. σ-Norms and Smooth Adjacency Elements

To construct a smooth collective potential of a flock and spatial adjacency matrix of a proximity net, we need to define a nonnegative map called a σ-norm.

The *σ-norm* of a vector is a map $\mathbb{R}^m \to \mathbb{R}_{\geq 0}$ (*not* a norm) defined as

$$\|z\|_\sigma = \frac{1}{\epsilon}[\sqrt{1 + \epsilon \|z\|^2} - 1] \tag{8}$$

with a parameter $\epsilon > 0$ and a gradient $\sigma_\epsilon(z) = \nabla\|z\|_\sigma$ given by

$$\sigma_\epsilon(z) = \frac{z}{\sqrt{1+\epsilon\|z\|^2}} = \frac{z}{1+\epsilon\|z\|_\sigma} \tag{9}$$

The parameter ϵ of the σ-norm remains fixed throughout the paper. One might wonder why we even need to define a new norm. The map $\|z\|_\sigma$ is differentiable everywhere, but $\|z\|$ is not differentiable at $z = 0$. Later, this property of σ-norms is used for construction of smooth collective potential functions for groups of particles.

A *bump function* is a scalar function $\rho_h(z)$ that smoothly varies between 0 and 1. Here, we use bump functions for construction of smooth potential functions with finite cut-offs and smooth adjacency matrices. One possible choice is the following bump function introduced in [44]:

$$\rho_h(z) = \begin{cases} 1, & z \in [0,h) \\ \frac{1}{2}\left[1+\cos\left(\pi\frac{(z-h)}{(1-h)}\right)\right], & z \in [h,1] \\ 0, & \text{otherwise} \end{cases} \tag{10}$$

where $h \in (0,1)$. One can show that $\rho_h(z)$ is a C^1-smooth function with the property that $\rho_h'(z) = 0$ over the interval $[1,\infty)$ and $|\rho_h'(z)|$ is uniformly bounded in z. Using this bump function, we can define a *spatial adjacency matrix* $A(q)$ via its elements by

$$a_{ij}(q) = \rho_h(\|q_j - q_i\|_\sigma / r_\alpha) \in [0,1], \qquad j \neq i \tag{11}$$

where $r_\alpha = \|r\|_\sigma$ and $a_{ii}(q) = 0$ for all i and q. For $h = 1, \rho_h(z)$ is an indicator function that is equal to 1 over the interval [0,1) and 0, otherwise. The use of an indicator bump function leads to a proximity net with 0-1 position-dependent adjacency elements.

D. Collective Potential Functions

The collective potential function $V(q)$ of a group of agents is a nonnegative function $V : \mathbb{R}^{mn} \to \mathbb{R}_{\geq 0}$ with the property that any solution of the set of algebraic constraints in (5) is "closely related to" a local minima of $V(q)$ and *vice versa*. In this paper, a collective potential is a smooth version of a deviation energy function with a scalar pairwise potential that has a *finite cut-off*. This feature turns out to be the fundamental source of scalability of our flocking algorithms.

Remark 2: Generalized Lennard–Jones functions and exponentially vanishing maps do not have finite cut-offs and are inadequate for our purpose without any modifications. A common approach to create a pairwise potential with a finite cut-off is "soft cutting" in which a pairwise potential is multiplied by a bump function.

Let $\psi(z) : \mathbb{R}_{\geq 0} \to \mathbb{R}_{\geq 0}$ be an *attractive/repulsive* pairwise potential with a global minimum at $z = d$ and a finite cut-off at r. Then, the following function:

$$\varphi(q) = \frac{1}{2}\sum_i \sum_{j\neq i} \psi(\|q_j - q_i\|) \tag{12}$$

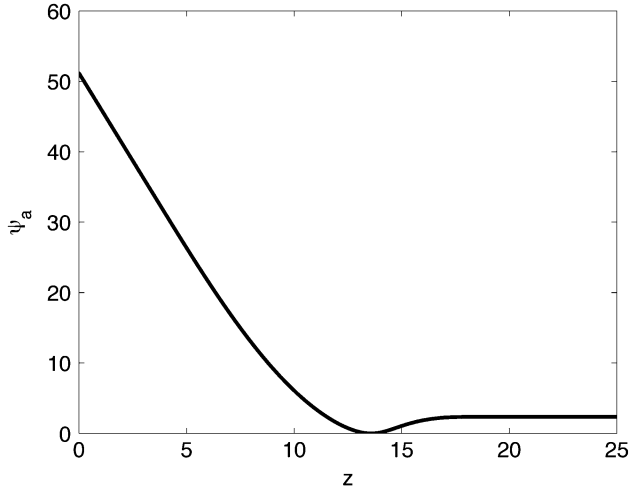

Fig. 3. Smooth pairwise potential $\psi_\alpha(z)$ with a finite cut-off.

is a collective potential that is not differentiable at singular configurations in which two distinct nodes coincide, or $q_i = q_j$. To resolve this problem, we use the set of algebraic constraints in (5) that are rewritten in terms of σ-norms as

$$\|q_j - q_i\|_\sigma = d_\alpha \qquad \forall j \in N_i(q) \tag{13}$$

where $d_\alpha = \|d\|_\sigma$. These constraints induce a *smooth collective potential function* in the form:

$$V(q) = \frac{1}{2}\sum_i \sum_{j\neq i} \psi_\alpha(\|q_j - q_i\|_\sigma) \tag{14}$$

where $\psi_\alpha(z)$ is a smooth pairwise attractive/repulsive potential (defined in (16)) with a finite cut-off at $r_\alpha = \|r\|_\sigma$ and a global minimum at $z = d_\alpha$.

To construct a smooth pairwise potential with finite cut-off, we integrate an action function $\phi_\alpha(z)$ that vanishes for all $z \geq r_\alpha$. Define this action function as

$$\begin{aligned} \phi_\alpha(z) &= \rho_h(z/r_\alpha)\phi(z - d_\alpha) \\ \phi(z) &= \frac{1}{2}[(a+b)\sigma_1(z+c) + (a-b)] \end{aligned} \tag{15}$$

where $\sigma_1(z) = z/\sqrt{1+z^2}$ and $\phi(z)$ is an uneven sigmoidal function with parameters that satisfy $0 < a \leq b, c = |a-b|/\sqrt{4ab}$ to guarantee $\phi(0) = 0$. The pairwise *attractive/repulsive potential* $\psi_\alpha(z)$ in (14) is defined as

$$\psi_\alpha(z) = \int_{d_\alpha}^{z} \phi_\alpha(s)\, ds. \tag{16}$$

This function is depicted in Fig. 3.

E. Consensus on Proximity Nets and Graph Laplacians

Graph Laplacians of proximity nets appear in analysis of velocity matching of agents in flocks. Consider a graph G of order n with adjacency matrix $A = [a_{ij}]$. The *degree matrix* of G is a diagonal matrix $\Delta = \Delta(A)$ with diagonal elements $\sum_{j=1}^n a_{ij}$

that are row-sums of A. The scalar *graph Laplacian* $L = [l_{ij}]$ is an $n \times n$ matrix associated with graph G that is defined as

$$L = \Delta(A) - A. \tag{17}$$

Laplacian matrix L always has a right eigenvector of $\mathbf{1}_n = (1, \ldots, 1)^T$ associated with eigenvalue $\lambda_1 = 0$. The following lemma summarizes the basic properties of graph Laplacians.

Lemma 1: Let $G = (\mathcal{V}, \mathcal{E})$ be an undirected graph of order n with a nonnegative adjacency matrix $A = A^T$. Then, the following statements hold.

i) L is a positive semidefinite matrix that satisfies the following sum-of-squares (SOS) property:

$$z^T L z = \frac{1}{2} \sum_{(i,j)\in\mathcal{E}} a_{ij}(z_j - z_i)^2, \qquad z \in \mathbb{R}^n. \tag{18}$$

ii) The graph G has $c \geq 1$ connected components iff $\text{rank}(L) = n - c$. Particularly, G is connected iff $\text{rank}(L) = n - 1$.

iii) Let G be a connected graph, then

$$\lambda_2(L) = \min_{z \perp \mathbf{1}_n} \frac{z^T L z}{\|z\|^2} > 0. \tag{19}$$

Proof: All three results are well-known in the field of algebraic graph theory and their proofs can be found in [48]. □

The quantity $\lambda_2(L)$ is known as *algebraic connectivity* of a graph [50]. In [21], it was shown that the speed of convergence of a linear consensus protocol is equal to $\lambda_2 > 0$. This consensus protocol will appear as a *velocity matching* term in all flocking algorithms that will be presented in this paper. Particularly, we use *m-dimensional graph Laplacians* defined by

$$\hat{L} = L \otimes I_m \tag{20}$$

where $\otimes$ denotes the Kronecker product. This mutli-dimensional Laplacian satisfies the following SOS property:

$$z^T \hat{L} z = \frac{1}{2} \sum_{(i,j)\in\mathcal{E}} a_{ij}\|z_j - z_i\|^2, \qquad z \in \mathbb{R}^{mn} \tag{21}$$

where $z = \text{col}(z_1, z_2, \ldots, z_n)$ and $z_i \in \mathbb{R}^m$ for all i. This property holds for a proximity net $G(q)$ as well.

III. Flocking Algorithms

In this section, we present a set of distributed algorithms for flocking in free-space, or *free-flocking*. We refer to a physical agent with dynamics $\ddot{q}_i = u_i$ as an *α-agent*. In nature, α-agents correspond to birds, bees, fish, and ants. Later, we introduce virtual agents called β-agents and γ-agents which model the effect of "obstacles" and "collective objective" of a group, respectively. The primary objective of an α-agent in a flock is to form an α-lattice with its neighboring α-agents.

In free-flocking, each α-agent applies a control input that consists of three terms

$$u_i = f_i^g + f_i^d + f_i^\gamma \tag{22}$$

where $f_i^g = -\nabla_{q_i} V(q)$ is a *gradient-based term*, f_i^d is a *velocity consensus term* that acts as a damping force, and f_i^γ is a navigational feedback due to a group objective. An example of a group objective is migration toward a destination. We propose two distributed algorithms that can be used for creation of flocking motion in $\mathbb{R}^m$ ($m = 1, 2, 3$ are of great interest).

Algorithm 1: $u_i = u_i^\alpha$ with

$$u_i^\alpha = \underbrace{\sum_{j\in N_i} \phi_\alpha(\|q_j - q_i\|_\sigma)\mathbf{n}_{ij}}_{\text{gradient-based term}} + \underbrace{\sum_{j\in N_i} a_{ij}(q)(p_j - p_i)}_{\text{consensus term}} \tag{23}$$

where $\mathbf{n}_{ij} = \sigma_\epsilon(q_j - q_i) = (q_j - q_i/\sqrt{1 + \epsilon\|q_j - q_i\|^2})$ is a vector along the line connecting q_i to q_j and $\epsilon \in (0, 1)$ is a *fixed* parameter of the σ-norm. Algorithm 1 has *no group objective* and is known as the (α, α) *protocol of flocking* [43] because it states the interaction rule between two α-agents. Later, we show that this algorithm embodies all three flocking rules of Reynolds.

Algorithm 2: $u_i = u_i^\alpha + u_i^\gamma$, or

$$u_i = \sum_{j\in N_i} \phi_\alpha(\|q_j - q_i\|_\sigma)\mathbf{n}_{ij} + \sum_{j\in N_i} a_{ij}(q)(p_j - p_i) + f_i^\gamma(q_i, p_i, q_r, p_r) \tag{24}$$

where u_i^γ is the *navigational feedback* and is given by

$$\begin{aligned} u_i^\gamma &:= f_i^\gamma(q_i, p_i, q_r, p_r) \\ &= -c_1(q_i - q_r) - c_2(p_i - p_r), \qquad c_1, c_2 > 0. \end{aligned}$$

The pair $(q_r, p_r) \in \mathbb{R}^m \times \mathbb{R}^m$ is the state of a γ-agent. A *γ-agent* is dynamic/static agent that represents a group objective and can be viewed as a *moving rendezvous point*. Let (q_d, p_d) be a fixed pair of m-vectors that denote the initial position and velocity of a γ-agent. A *dynamic γ-agent* has the following model:

$$\begin{cases} \dot{q}_r = p_r \\ \dot{p}_r = f_r(q_r, p_r) \end{cases} \tag{25}$$

with $(q_r(0), p_r(0)) = (q_d, p_d)$. A *static γ-agent* has a fixed state that is equal to (q_d, p_d) for all time. The design of $f_r(q_r, p_r)$ for a dynamic γ-agent is part of tracking control design for a group of agents. For example, the choice of $f_r \equiv 0$ leads to a γ-agent that moves along a straight line with a desired velocity p_d. Based on expression of u_i^γ, a *secondary objective* of an α-agent is to track a γ-agent.

We shall see that despite the similarities between certain terms in these protocols, *the collective behavior of a group of agents that use Algorithm 1 is drastically different than a group of agents applying Algorithm 2*.

It turns out that protocol (23) leads to flocking behavior only for a *very restricted set of initial states*. For generic set of initial states and large number of agents (e.g., $n > 10$), protocol (23) most likely fails to produce flocking behavior and instead leads to *regular fragmentation* as illustrated in Fig. 4. Fragmentation is a pitfall of flocking. In contrast, protocol (24) never leads to fragmentation. The importance of Algorithm 1 is due to its fundamental role in forming lattice-shape structures during flocking as a key element of Algorithm 2.

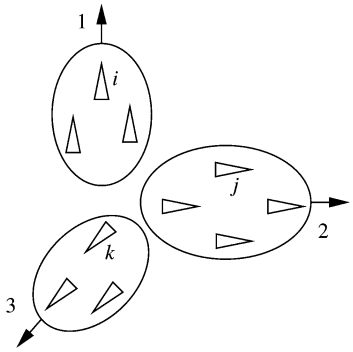

Fig. 4. Fragmentation phenomenon.

IV. Collective Dynamics

The *collective dynamics* of a group of α-agents applying protocol (24) is in the form

$$\begin{cases} \dot{q} = p \\ \dot{p} = -\nabla V(q) - \hat{L}(q)p + f_\gamma(q, p, q_r, p_r) \end{cases} \tag{26}$$

where $V(q)$ is a smooth collective potential function given in (14) and $\hat{L}(q)$ is the m-dimensional Laplacian of the proximity net $G(q)$ with a state-dependent adjacency matrix $A(q) = [a_{ij}(q)]$. Note that for Algorithm 1, $f_\gamma \equiv 0$.

The first expected result is that with $f_\gamma \equiv 0$, system (26) is a *dissipative particle system* with Hamiltonian

$$H(q, p) = V(q) + \sum_{i=1}^{n} \|p_i\|^2. \tag{27}$$

This is due to $\dot{H} = -p^T \hat{L}(q)p \leq 0$ and the fact that the multi-dimensional graph Laplacian $\hat{L}(q)$ is a positive semidefinite matrix for all q.

The key in stability analysis of collective dynamics is employing a correct coordinate system that allows the use of LaSalle's invariance principle. The naive approach is to use $H(q, p)$ in the (q, p)-coordinates. The reason such an approach does not work (for most cases of interest) is that one cannot establish the boundedness of solutions. During fragmentation, the solution cannot remain bounded. Therefore, we propose the use of a *moving frame* to analyze the stability of flocking motion as suggested in [43].

Consider a moving fame that is centered at q_c—the center of mass (CM) of all particles. Let $\mathrm{Ave}(z) = (1/n)\sum_{i=1}^{n} z_i$ denote the average of the z_i's with $z = \mathrm{col}(z_1, \ldots, z_n)$. Let $q_c = \mathrm{Ave}(q)$ and $p_c = \mathrm{Ave}(p)$ denote the position and velocity of the origin of the moving frame. Then $\dot{q}_c(t) = p_c(t)$ and $\dot{p}_c(t) = \mathrm{Ave}(u(t))$. The position and velocity of agent i in the moving frame is given by

$$\begin{cases} x_i = q_i - q_c \\ v_i = p_i - p_c. \end{cases} \tag{28}$$

The relative positions and velocities remain the same in the moving frame, i.e., $x_j - x_i = q_j - q_i$ and $v_j - v_i = p_j - p_i$. Thus, $V(q) = V(x)$ and $\nabla V(q) = \nabla V(x)$. The (α, α) protocol in the moving frame can be expressed as

$$u_i^\alpha = \sum_{j \in N_i} \phi_\alpha(\|x_j - x_i\|_\sigma)\mathbf{n}_{ij} + \sum_{j \in N_i} a_{ij}(x)(v_j - v_i)$$

with $a_{ij}(x) = \rho_h(\|x_j - x_i\|_\sigma / r_\alpha)$. Our first result is a decomposition lemma that is the basis for posing a structural stability problem for the motion of flocks.

Lemma 2 (Decomposition): Suppose that the navigational feedback $f_\gamma(q, p)$ is linear, i.e., there exists a decomposition of $f_\gamma(q, p)$ in the following form:

$$f_\gamma(q, p, q_r, p_r) = g(x, v) + \mathbf{1}_n \otimes h(q_c, p_c, q_r, p_r). \tag{29}$$

Then, the collective dynamics of a group of agents applying protocol (24) [or (23)] can be decomposed as n second-order systems in the moving frame

$$\text{structural dyn.} : \begin{cases} \dot{x} = v \\ \dot{v} = -\nabla V(x) - \hat{L}(x)v + g(x, v) \end{cases} \tag{30}$$

and one second-order system in the reference frame

$$\text{translational dyn.} : \begin{cases} \dot{q}_c = p_c \\ \dot{p}_c = h(q_c, p_c, q_r, p_r) \end{cases} \tag{31}$$

where

$$\begin{aligned} g(x, v) &= -c_1 x - c_2 v \\ h(q_c, p_c, q_r, p_r) &= -c_1(q_c - q_r) - c_2(p_c - p_r) \end{aligned} \tag{32}$$

and (q_r, p_r) is the state of the γ-agent.

Proof: See [51, App. A]. □

A discussion of the effects of using a nonlinear navigational feedback is presented in [51, App. B]. In this case, it turns out that the structural and translational dynamics are coupled.

V. Stability Analysis of Flocking

According to the decomposition lemma, we are now at the position to define *stable flocking motion* as the combination of the following forms of stability properties: 1) stability of certain equilibria of the structural dynamics, and 2) stability of a desired equilibrium of the translational dynamics. The challenge in analysis of flocking behavior is to establish part 1.

The significant differences in group behaviors created by Algorithms 1 and 2 are due to the considerable differences in the structural dynamics induced by the two algorithms. Given Algorithm 1, one obtains the following structural dynamics:

$$\Sigma_1 : \begin{cases} \dot{x} = v \\ \dot{v} = -\nabla V(x) - \hat{L}(x)v \end{cases} \tag{33}$$

with a *positive semidefinite* Laplacian matrix $\hat{L}(x)$. In comparison, the structural dynamics of a group of agents applying Algorithm 2 is in the form

$$\Sigma_2 : \begin{cases} \dot{x} = v \\ \dot{v} = -\nabla U_\lambda(x) - D(x)v \end{cases} \tag{34}$$

where $U_\lambda(x)$ is called the *aggregate potential function* and is defined by

$$U_\lambda(x) = V(x) + \lambda J(x). \tag{35}$$

The map $J(x) = (1/2)\sum_{i=1}^{n} \|x_i\|^2$ is the *moment of inertia* of all particles and $\lambda = c_1 > 0$ is a parameter of the navigational feedback. Moreover, the damping matrix $D(x) = c_2 I_m + \hat{L}(x)$ is a *positive definite* matrix with $c_2 > 0$.

Before presenting the stability analysis of flocking behavior under Algorithms 1 and 2, we need to define the structural Hamiltonians of systems Σ_1 and Σ_2 as follows:

$$\begin{aligned} H(x,v) &= V(x) + K(v) \\ H_\lambda(x,v) &= U_\lambda(x) + K(v) \end{aligned} \tag{36}$$

where $K(v) = (1/2)\sum_i \|v_i\|^2$ is the velocity mismatch function, or the kinetic energy of the particle system in the moving frame. We also need to define what we mean by "cohesion of a group" and "flocks."

Definition 2 (A Cohesive Group): Let $(q(\cdot), p(\cdot)) : t \mapsto \mathbb{R}^{mn} \times \mathbb{R}^{mn}$ be the state trajectory of a group of dynamic agents over the time interval $[t_0, t_f]$. We say the group is *cohesive* for all $t \in [t_0, t_f]$ if there exists a ball of radius $R > 0$ centered at $q_c(t) = \text{Ave}(q(t))$ that contains all the agents for all time $t \in [t_0, t_f]$, i.e., $\exists R > 0 : \|x(t)\| \leq R, \forall t \in [t_0, t_f]$.

Definition 3 (Flocks): A group of α-agents is called a *flock* over the interval $[t_0, t_f)$ if the proximity net $G(q(t))$ is connected over $[t_0, t_f)$ $(t_f \geq t_0)$.

The group is called a *quasi-flock* if the largest component of the proximity net is highly populated. The following lemma provides a geometric characterization of the set of local minima of the collective potential and plays a critical role in establishing the *spatial-order of self-organizing flocks*.

Lemma 3. (Spatial-Order): Every local minima of $V(q)$ is an α-lattice and *vice versa*.

Proof: Define an *ε-neighborhood of q* as

$$\mathcal{N}_\varepsilon(q) = \{q' \in \mathbb{R}^{mn} : \|q_i' - q_i\| \leq \varepsilon \qquad \forall i \in \mathcal{V}\} \tag{37}$$

where $q' = \text{col}(q_1', q_2', \ldots, q_n')$. A configuration q^* is called a *local minima* of $V(q)$ if there exists an ϵ-neighborhood $\mathcal{N}_\varepsilon(q)$ of q^* such that $V(q) \geq V(q^*)$ for all $q \in \mathcal{N}_\varepsilon(q^*)$. Keep in mind that $V(q)$ remains invariant under rotation and translation of all q_i's, therefore, it does not have any *isolated* local minima.

The collective potential function $V(q)$ can be decomposed into two terms: A graph-induced potential function by the proximity net $G(q)$ and an additional term that is an integer factor of $h_0 = \psi_\alpha(r_\alpha)$, i.e.,

$$V(q) = V_G(q) + k(q)h_0 \tag{38}$$

where

$$\begin{aligned} V_G(q) &= \frac{1}{2}\sum_{(i,j)\in\mathcal{E}(q)} \psi_\alpha(\|q_j - q_i\|_\sigma) \\ k(q) &= \frac{1}{2}(n(n-1) - |\mathcal{E}(q)|) \in \mathcal{I} \end{aligned} \tag{39}$$

with $\mathcal{I} = \{0, 1, \ldots, n(n-1)\}$. Notice that $k(q)$ is an integer that is directly determined by the number of edges of the proximity net $G(q)$ ((i,j) and (j,i) with $i \neq j$ count as two edges). The higher the size of the proximity net $G(q)$, the lower the value of $k(q)$. Let Q_k denote the set of configurations that induce proximity nets with $|\mathcal{E}(q)| = n(n-1) - 2k$ edges for a fixed specification (d, r). Observe that $\cup_{k=0}^{n(n-1)} Q_k = \mathbb{R}^{mn}$. For a fixed $k \in \mathcal{I}$, we have

$$V(q) = V_G(q) + kh_0 \geq kh_0 \tag{40}$$

for all $q \in Q_k$. Any configuration q^* that achieves the equality in (40) is a local minima of $V(q)$ and satisfies $V_G(q^*) = 0$. On the other hand, $\psi_\alpha(z)$ takes the value zero only at $z = d_\alpha$, hence, the configuration q^* satisfies

$$\|q_j^* - q_i^*\|_\sigma = d_\alpha \Longrightarrow \|q_j^* - q_i^*\| = d$$

for all $j \in N_i(q)$. This means that q^* is an α-lattice. The proof of the converse is rather similar and is omitted. □

Theorem 1: Consider a group of α-agents applying protocol (23) (Algorithm 1) with structural dynamics Σ_1 (defined in (33)). Let $\Omega_c = \{(x,v) : H(x,v) \leq c\}$ be a level-set of the Hamiltonian $H(x,v)$ of Σ_1 such that for any solution starting in Ω_c, the agents form a cohesive flock $\forall t \geq 0$. Then, the following statements hold.

i) Almost every solution of the structural dynamics converges to an equilibrium $(x^*, 0)$ with a configuration x^* that is an α-lattice.
ii) All agents asymptotically move with the same velocity.
iii) Given $c < c^* = \psi_\alpha(0)$, no interagent collisions occur for all $t \geq 0$.

Proof: Any solution $(q(t), p(t))$ of the collective dynamics of α-agents applying protocol (23) is uniquely mapped to a solution $(x(t), v(t))$ of the structural dynamics Σ_1. We have

$$\dot{H}(x,v) = -v^T \hat{L}(x) v = -\frac{1}{2}\sum_{(i,j)\in\mathcal{E}(x)} a_{ij}(x)\|v_j - v_i\|^2 \leq 0 \tag{41}$$

which means the structural energy $H(x,v)$ is monotonically decreasing for all $t \geq 0$. In addition, $H(x(t), v(t)) \leq c$ for all $t \geq 0$ that implies Ω_c is an invariant set. This guarantees that the velocity mismatch is upper bounded by c because of

$$K(v(t)) \leq H(x(t), v(t)) \leq c \qquad \forall t \geq 0.$$

By assumption, for any solution starting in Ω_c, the group is cohesive in all time $t \geq 0$. Hence, there exists an $R > 0$ such that $\|x(t)\| \leq R, \forall t \geq 0$. The combination of boundedness of velocity mismatch and group cohesion guarantees boundedness of solutions of Σ_1 starting in Ω_c. This fact is the result of the following inequality:

$$\|(x(t), v(t))\|^2 := \|x(t)\|^2 + \|v(t)\|^2 \leq R^2 + 2c =: C \tag{42}$$

where $C > 0$ is a constant.

From LaSalle's invariance principle, all the solutions of Σ_1 starting in Ω_c converge to the largest invariant set in $E = \{(x,v) \in \Omega_c : \dot{H} = 0\}$. However, since the group of α-agents constitutes a dynamic flock for all $t \geq 0, G(q(t))$ is a connected graph for all $t \geq 0$. Thus, based on (41), we conclude that the velocities of all agents match in the moving

frame, or $v_1 = \ldots = v_n$. However, $\sum_i v_i = 0$, therefore, $v_i = 0$ for all i (or $v = 0$). This means that the velocity of all agents asymptotically match in the reference frame, or $p_1 = p_2 = \ldots = p_n$, which proves part ii). Moreover, the configuration x asymptotically converges to a fixed configuration x^* that is an exterma of $V(x)$, i.e., $\nabla V(x^*) = 0$.

Since any solution of the system starting at certain equilibria such as local maxima or saddle points remain in those equilibria for all time, not all solutions of the system converge to a local minima. However, anything but a local minima is an unstable equilibria (a blanket assumption). Thus, almost every solution of the system converges to an equilibrium $(x^*, 0)$ where x^* is a local minima of $V(x)$. According to Lemma 3, every local minima of $V(x)$ is an α-lattice. Therefore, x^* is an α-lattice and asymptotically all inter-agent distances between neighboring α-agents become equal to d. This finishes the proof of parts i) and ii).

We prove part iii) by contradiction. Assume there exists a time $t = t_1 > 0$ so that two distinct agents k, l collide, or $q_k(t_1) = q_l(t_1)$. For all $t \geq 0$, we have

$$\begin{aligned} V(q(t)) &= \frac{1}{2}\sum_i \sum_{j\neq i} \psi_\alpha(\|q_j - q_i\|_\sigma) \\ &= \psi_\alpha(\|q_k(t) - q_l(t)\|_\sigma) \\ &\quad + \frac{1}{2}\sum_{i\in\mathcal{V}\setminus\{k,l\}} \sum_{j\in\mathcal{V}\setminus\{i,k,l\}} \psi_\alpha(\|q_j - q_i\|_\sigma) \\ &\geq \psi_\alpha(\|q_k(t) - q_l(t)\|_\sigma). \end{aligned}$$

Hence, $V(q(t_1)) \geq \psi_\alpha(0) =: c^*$. But the velocity mismatch is a nonnegative quantity and Ω_c is an invariant level-set of H. Thus

$$V(q(t)) \leq H(x(t), v(t)) - K(v(t)) \leq H(x(t), v(t)) \leq c < c^*$$

for all $t \geq 0$. This is in contradiction with an earlier inequality $V(q(t_1)) \geq c^*$. Therefore, no two agents collide at any time $t \geq 0$. □

The assumptions in Theorem 1 rarely hold for a generic set of initial states and thus fragmentation emerges instead of flocking. In contrast, the assumptions of the following theorem hold for generic set of initial states without any necessity to presume group cohesion or connectivity of the proximity net of the agents over and infinite time interval.

Theorem 2: Consider a group of α-agents applying protocol (24) (Algorithm 2) with $c_1, c_2 > 0$ and structural dynamics Σ_2 [defined in (34)]. Assume that the initial velocity mismatch $K(v(0))$ and inertia $J(x(0))$ are finite. Then, the following statements hold.

i) The group of agents remain cohesive for all $t \geq 0$.
ii) Almost every solution of Σ_2 asymptotically converges to an equilibrium point $(x^*_\lambda, 0)$ where x^*_λ is a local minima of $U_\lambda(x)$.
iii) All agents asymptotically move with the same velocity.
iv) Assume the initial structural energy of the particle system is less than $(k+1)c^*$ with $c^* = \psi_\alpha(0)$ and $k \in \mathbb{Z}_+$. Then, at most k distinct pairs of α-agents could possibly collide ($k = 0$ guarantees a collision-free motion).

Proof: First, note that the particle system with structural dynamics Σ_2 and Hamiltonian $H_\lambda(x, v) = U_\lambda(x) + K(v)$ is a strictly dissipative particle system in the moving frame because it satisfies

$$\dot{H}_\lambda(x, v) = -v^T(c_2 I_m + \hat{L}(x))v = -c_2(v^T v) - v^T \hat{L}(x)v < 0$$

for all $v \neq 0$. Hence, the structural energy $H_\lambda(x, v)$ is monotonically decreasing for all (x, v) and

$$H_\lambda(x(t), v(t)) \leq H_0 := H_\lambda(x(0), v(0)) < \infty.$$

The finiteness of $H_0 = V(x(0)) + \lambda J(x(0)) + K(v(0))$ follows from the assumption that the collective potential, the inertia, and the velocity mismatch are all initially finite. Thus, for all $t \geq 0$, we have

$$U_\lambda(x(t)) \leq H_0, K(v(t)) \leq H_0.$$

However, $U_\lambda(x) = V(x) + (\lambda/2)x^T x$ with $\lambda > 0$ and $V(x) \geq 0$ for all x, therefore

$$x^T(t)x(t) \leq \frac{2H_0}{\lambda} \qquad \forall t \geq 0.$$

This guarantees the cohesion of the group of α-agents for all $t \geq 0$ because the position of all agents remains in a ball of radius $R = \sqrt{2H_0/\lambda}$ centered at q_c. This cohesion property together with boundedness of velocity mismatch, or $K(v(t)) \leq H_0$, guarantees boundedness of solutions of the structural dynamics Σ_2. To see this, let $z = \mathrm{col}(x, v)$, then

$$\begin{aligned} \|z(t)\|^2 &= x^T(t)x(t) + v^T(t)v(t) \\ &\leq 2\left(\frac{1}{\lambda} + 1\right) H_0 =: C(\lambda) < \infty. \end{aligned}$$

Part ii) follows from LaSalle's invariance principle. Keep in mind that $\dot{H}_\lambda(x, v) = 0$ implies $v = 0$. Thus, similar to the argument in the proof of Theorem 1, almost every solution of the particle system asymptotically converges to an equilibrium point $z^*_\lambda = (x^*_\lambda, 0)$ where x^*_λ is a local minima of the aggregate potential function $U_\lambda(x)$.

Part iii) follows from the fact that v asymptotically vanishes. Thus, the velocities of all agents asymptotically match in the reference frame.

To prove part iv), suppose $H_0 < (k+1)c^*$ and there are more than k distinct pairs of agents that collide at a given time $t_1 \geq 0$. Hence, there must be at least $k+1$ distinct pairs of agents that collide at time t_1. This implies the collective potential of the particle system at time $t = t_1$ is at least $(k+1)\psi_\alpha(0)$. However, we have

$$\begin{aligned} H_0 &= V(x(0)) + \lambda J(x(0)) + K(v(0)) \geq V(x(0) \\ &\geq (k+1)\psi_\alpha(0). \end{aligned}$$

This contradicts the assumption that $H_0 < (k+1)c^*$. Hence, no more than k distinct pairs of agents can possibly collide at any time $t \geq 0$. Finally, with $k = 0$, no two agents ever collide. □

Theorem 2 establishes some critical properties of collective behavior of a group of agents applying Algorithm 2 including cohesion, convergence, asymptotic velocity matching, and collision-avoidance. But, unless one provides a geometric characterization of local minima of $U_\lambda(q)$ for relatively small $\lambda > 0$, it is not possible to establish that the limiting conformation x^*_λ is "closely related" to an α-lattice. I would like to pose two conjectures that establish this close relationship between geometric and graph theoretic properties of any local minima of $U_\lambda(q)$ and features of flocks.

Conjecture 1 (Connectivity): Any local minima q^*_λ of $U_\lambda(q)$ for $\lambda > 0$ induces a connected proximity net.

The implication of Conjecture 1 is that a flock of α-agents is asymptotically self-assembled. The next conjecture states geometric properties of q^*_λ.

Conjecture 2 (Quasi α-Lattice): Let $U_\lambda(q) = V(q) + \lambda J(x)$ be an aggregate potential function with parameter $\lambda > 0$. For any fixed n, d, r satisfying $r/d = 1 + \varepsilon$ ($\varepsilon \ll 1$), there exists a $\lambda^* \ll 1$ so that 1) any local minima q^*_λ of $U_\lambda(q)$ with $\lambda \in (0, \lambda^*)$ is a quasi α-lattice with ratio $\kappa = 1+\varepsilon$ and 2) q^*_λ induces a planar graph $(G(q^*_\lambda), q^*_\lambda)$ in dimensions $m = 1, 2, 3$.

Proof/disproof of both conjectures is the subject of ongoing research. Now, we are ready to present a more enhanced version of Theorem 2 with both geometric and graph theoretic relations to flocking.

Theorem 3: Consider a group of α-agents applying protocol (24) (Algorithm 2) with $c_1, c_2 > 0$ and structural dynamics Σ_2. Assume the initial structural energy is finite and the interaction range satisfies $r/d = 1 + \varepsilon$ ($\varepsilon \ll 1$). If Conjectures 1 and 2 hold, then almost every solution of Σ_2 asymptotically converges to an equilibrium point $(x^*_\lambda, 0)$ where x^*_λ is a quasi-α-lattice and a flock is asymptotically self-assembled.

Proof: The proof follows from part ii) of Theorem 2 and Conjectures 1 and 2. □

In simulation results of flocking (see Section VIII), the author observed that during flocking, the proximity structures induced by the trajectory of α-agents were planar graphs. The following theorem, analytically establishes this planarity property as well as a bound on the computational complexity of proximity nets induced by α-lattices.

Theorem 4 (Planarity): Let q be an α-lattice of scale $d > 0$ and ratio $\kappa > 1$ with n nodes at distinct positions. Then

i) the proximity structure $(G(q), q)$ is a planar graph in dimensions $m = 2, 3$;
ii) the proximity net $G(q)$ has at most $3n - 6$ links in $\mathbb{R}^2$;
iii) the proximity net $G(q)$ with $n > m + 1$ nodes cannot be a complete graph in $\mathbb{R}^m$ for $m = 1, 2, 3$.

Proof: See [51, App. A]. □

The importance of *planarity* of the proximity structure $(G(q), q)$ in 2-D space is that the total number of interaction terms for maintaining flocking motion is $O(n)$ (linear in the number of agents). This is a substantial reduction is computational complexity due to use of a distributed flocking algorithm compared to an $O(n^2)$ cost of implementation of all-to-all interaction topologies in some existing models of swarms.

Remark 3: According to Theorem 4, the planarity of graphs induced by α-lattices imposes a restriction on maximum ratio of the interaction range r to desired distance $d > 0$. For example, a cubic lattice q in dimension m is a valid α-lattice with ratio $\kappa = 1 + \varepsilon$ if $0 < \epsilon < \sqrt{m}$. Otherwise, two nodes that are on opposite sides of the diagonal of a hypercube become neighbors and this invalidates q as an α-lattice. Since each node can no longer be equally distanced from all of its neighbors.

VI. Algorithm 1 Embodies Reynolds Rules

In this section, we demonstrate that Algorithm 1embodies extended forms of all three rules of Reynolds [5] in a single equation. The main ambiguity of Reynolds rules is that it is unclear when and how each rule applies since none of the rules are mathematically stated. This issue is resolved during our attempt to extract Reynolds rules formally from Algorithm 1.

The key tool in our analysis are *stress elements of a graph* [44]. Let us define the stress elements associated with edge (i, j) of the proximity net $G(q)$ as

$$s_{ij}(q) = \frac{\phi_\alpha(\|q_j - q_i\|_\sigma)}{1 + \epsilon\|q_j - q_i\|_\sigma}, \qquad (i, j) \in \mathcal{E}(q). \tag{43}$$

The stress elements between nonneighboring agents are defined to be zero. The (α, α) flocking protocol can be expressed in terms of stress and adjacency elements as follows:

$$\begin{aligned} u^\alpha_i &= \sum_{j \in N_i(q)} s_{ij}(q)(q_j - q_i) + \sum_{j \in N_i(q)} a_{ij}(q)(p_j - p_i) \\ &= u^g_i + u^d_i. \end{aligned}$$

From the previous equation, all three rules of Reynolds follow. The second term represents the velocity matching rule (or rule 3) and the first term embodies both the flock centering and separation rules (rules 1 and 2).

To demonstrate this fact, let us define $S_i(q) = \sum_{j \in N_i} s_{ij}(q)$. We have

$$u^g_i = \sum_{j \in N_i} s_{ij}(q)(q_j - q_i) = S_i(q)(q_i - \langle q_i \rangle) \tag{44}$$

where $\langle q_i \rangle$ is the weighted average of the position of the neighbors of agent i, i.e., $\langle q_i \rangle = (\sum_{j \in N_i} s_{ij}(q) q_j)/(\sum_{j \in N_i} s_{ij}(q))$. Hence, each agent obeys the following rules: a) if $S_i(q) > 0$, move toward the weighted center of the neighbors, and b) if $S_i(q) < 0$ move away from the weighted center of the neighbors. This together with velocity consensus term completes the proof of the claim that all three rules of Reynolds follow from Algorithm 1. Therefore, Reynolds rules are *insufficient* for creation of flocking behavior. Further details can be found in [51].

VII. Flocking With Obstacle Avoidance

In this section, we present a distributed flocking algorithm with multiple obstacle-avoidance capability. The main idea is to

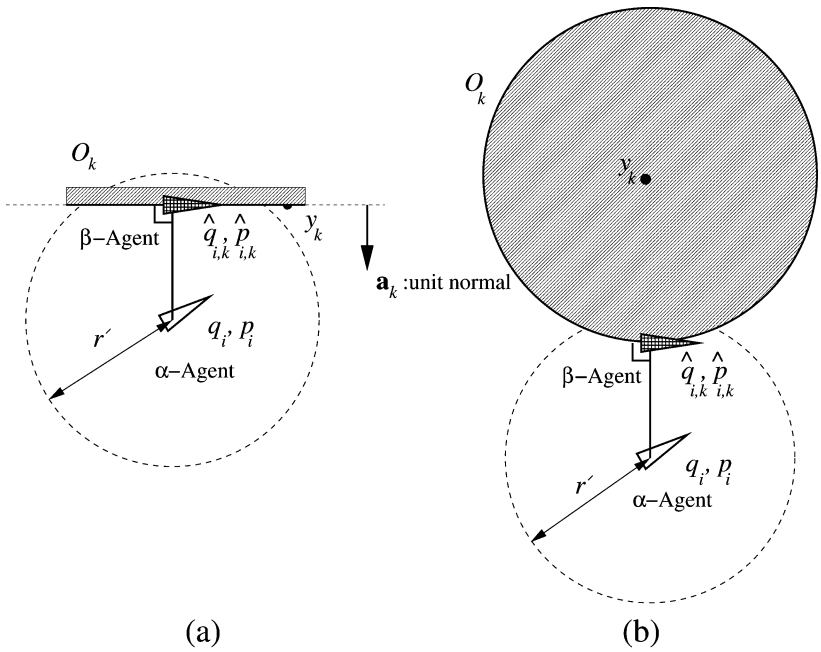

Fig. 5. Agent-based representation of obstacles. (a) Wall. (b) Spherical obstacle.

use agent-based representation of all nearby (active) obstacles by creating a new species of agents called β-agents. A *β-agent* is a kinematic agent that is induced by an α-agent whenever the α-agent is in close proximity of an obstacle. In the following, we formally define the notion of a β-agent and specify the interaction protocol between an α-agent and a β-agent.

We restrict our study to obstacles that are *connected convex regions* in $\mathbb{R}^m$ with boundaries that are smooth manifolds. Specifically, we focus on obstacles that are either spheres or infinite walls as shown in Fig. 5. Our approach to obstacle avoidance can be summarized in the following steps.

1) Determine the indices N_i^β (to be defined) of the set of obstacles O_k that are neighbors of α-agent i.
2) Create a (virtual) kinematic β-agent at $\hat{q}_{i,k}$ on the boundary of a neighboring obstacle O_k by projection where $\hat{q}_{i,k}$ satisfies
$$\hat{q}_{i,k} = \operatorname{argmin}_{x \in O_k} \|x - q_i\| \tag{45}$$
and O_k is either a closed ball or a closed half space on one side of a hyperplane.
3) Add a term $\psi_\beta(\|\hat{q}_{i,k} - q_i\|_\sigma)$ to the potential function of a group of α-agents corresponding to each β-agent at $\hat{q}_{i,k}$ ($\psi_\beta(z)$ to be defined).

This approach is partially motivated by the work of Khatib [38] and Helbing *et al.* [10]. Fig. 5 schematically illustrates the position of a β-agent induced by an α-agent in proximity of two types of obstacles. It is not difficult to imagine that notions such as proximity nets, proximity structures, and α-lattices can be generalized to their similar counterparts in presence of obstacles.

A. β-Neighbors of α-Agents: (α, β) Proximity Nets

Let $\mathcal{V}_\alpha = \{1, 2, \ldots, n\}$ and $\mathcal{V}_\beta = \{1', 2', \ldots, l'\}$ denote the set of indices of α-agents and obstacles (or β-agents), respectively. Notice that the prime in elements of $\mathcal{V}_\beta$ is used to guarantee that $\mathcal{V}_\alpha \cap \mathcal{V}_\beta = \emptyset$. An α-agent is called a *neighbor of an obstacle* O_k ($k \in \mathcal{V}_\beta$) if and only if the ball $B_{r'}(q_i)$ and O_k overlap (as shown in Fig. 5). This form of neighborhood between an α-agent and an obstacle is a mutual property. Moreover, an α-agent could possibly have multiple neighboring obstacles. Particularly, this occurs when a group of agents intend to pass through a narrow pathway.

We define the set of α-neighbors and β-neighbors of an α-agent $i \in \mathcal{V}_\alpha$ as follows:

$$N_i^\alpha = \{j \in \mathcal{V}_\alpha : \|q_j - q_i\| < r\} \tag{46}$$
$$N_i^\beta = \{k \in \mathcal{V}_\beta : \|\hat{q}_{i,k} - q_i\| < r'\} \tag{47}$$

where $r, r' > 0$ are *interaction ranges* of an α-agent with neighboring α-agents and β-agents, respectively. Here, we choose $r' < r$, but in general, r and r' can be chosen independently.

The sets of α- and β-neighbors of an α-agent $i \in \mathcal{V}_\alpha$ naturally define an (α, β) *proximity net* that is a spatially induced graph in the form

$$G_{\alpha,\beta}(q) = G_\alpha(q) + G_\beta(q) \tag{48}$$

where $G_\alpha(q) = (\mathcal{V}_\alpha, \mathcal{E}_\alpha(q))$ is a proximity net of all α-agents and $G_\beta(q) = (\mathcal{V}_\beta, \mathcal{E}_\beta(q))$ is a *directed bipartite graph* induced by q and the set of obstacles $\mathcal{O} = \{O_\|\colon \|\in \mathcal{V}_\beta\}$ where $\mathcal{E}_\beta(q) \subseteq \mathcal{V}_\alpha \times \mathcal{V}_\beta$. The condition $\mathcal{V}_\alpha \cap \mathcal{V}_\beta = \emptyset$ guarantees well-posedness of the definition of the bipartite graph $G_\beta(q)$. More explicitly, we have

$$\begin{aligned} \mathcal{E}_\alpha(q) &= \{(i,j) : i \in \mathcal{V}_\alpha, j \in N_i^\alpha\} \\ \mathcal{E}_\beta(q) &= \left\{(i,k) : i \in \mathcal{V}_\alpha, k \in N_i^\beta\right\} \end{aligned} \tag{49}$$

and $G_{\alpha,\beta}(q) = (\mathcal{V}_\alpha \cup V_\beta, \mathcal{E}_\alpha(q) \cup \mathcal{E}_\beta(q))$. Similarly, an (α, β) *proximity structure* is a triplet $(G_{\alpha,\beta}(q), q, \hat{q})$ where $\hat{q}$ denotes the configuration of all β-agents. Keep in mind that there are no edges between two β-agents.z

The new set of interagent and agent-to-obstacle algebraic constraints for an α-agent can be specified as follows:

$$\begin{cases} \|q_j - q_i\| = d & \forall j \in N_i^\alpha \\ \|\hat{q}_{i,k} - q_i\| = d' & \forall k \in N_i^\beta. \end{cases} \tag{50}$$

A *constrained α-lattice* denoted by $(q, \mathcal{O})$ consists of an α-lattice q and a set of obstacles $\mathcal{O}$ that satisfy the set of constraints in (50). The relevant ratios of a constrained α-lattice are $\kappa = r/d$ and $\kappa' = d'/d = r'/r$ (we assume $\kappa' = \kappa$).

B. Multispecies Collective Potentials

To achieve flocking in presence of obstacles, we use the following *mutli-species collective potential function* for the particle system:

$$V(q) = c_1^\alpha V_\alpha(q) + c_1^\beta V_\beta(q) + c_1^\gamma V_\gamma(q) \tag{51}$$

where the $c_1^\alpha, c_1^\beta, c_1^\gamma$ are positive constants and $(\alpha,\alpha), (\alpha,\beta), (\alpha,\gamma)$ interaction potentials are defined as follows:

$$V_\alpha(q) = \sum_{i \in \mathcal{V}_\alpha} \sum_{j \in \mathcal{V}_\alpha \setminus \{i\}} \psi_\alpha(\|q_j - q_i\|_\sigma) \tag{52}$$

$$V_\beta(q) = \sum_{i \in \mathcal{V}_\alpha} \sum_{k \in N_i^\beta} \psi_\beta(\|\hat{q}_{i,k} - q_i\|_\sigma) \tag{53}$$

$$V_\gamma(q) = \sum_{i \in \mathcal{V}_\alpha} (\sqrt{1 + \|q_i - q_r\|^2} - 1). \tag{54}$$

The function $V_\gamma(q)$ has to do with the navigational objective of a group of α-agents. The *heterogeneous adjacency* between an α-agent at q_i and its neighboring β-agent at $\hat{q}_{i,k}$ is defined as

$$b_{i,k}(q) = \rho_h(\|\hat{q}_{i,k} - q_i\|_\sigma / d_\beta) \tag{55}$$

where $d_\beta < r_\beta$ with $d_\beta = \|d'\|_\sigma, r_\beta = \|r'\|_\sigma$. Define the *repulsive action function*

$$\phi_\beta(z) = \rho_h(z/d_\beta)(\sigma_1(z - d_\beta) - 1) \tag{56}$$

with $\sigma_1(z) = z/\sqrt{1+z^2}$. Notice that $\phi_\beta(z)$ vanishes smoothly to zero at $z = d_\beta$ and remains zero for all $z \geq d_\beta$. This naturally defines a *repulsive pairwise potential* $\psi_\beta(z)$ in the form

$$\psi_\beta(z) = \int_{d_\beta}^{z} \phi_\beta(s) ds \geq 0. \tag{57}$$

Since vehicles/robots/animals in real-life cannot apply unbounded forces, we avoid the use of functions with unbounded derivatives such as $1/z$ or $\log(z)$. Clearly, $-2 < \psi'_\beta(z) \leq 0$ for all $z \in \mathbb{R}$, and thereby the derivative of $\psi_\beta(z)$ is uniformly bounded.

C. Flocking With Obstacle Avoidance

We are ready to present our main flocking algorithm with the capability to perform obstacle avoidance:

Algorithm 3: This algorithm consists of three terms

$$u_i = u_i^\alpha + u_i^\beta + u_i^\gamma \tag{58}$$

where u_i^α denotes the (α,α) interaction terms, u_i^β denotes the (α,β) interaction terms, and u_i^γ is a distributed navigational feedback. Each term in (58) is explicitly specified as follows:

$$\begin{aligned} u_i^\alpha &= c_1^\alpha \sum_{j \in N_i^\alpha} \phi_\alpha(\|q_j - q_i\|_\sigma) \mathbf{n}_{i,j} \\ &\quad + c_2^\alpha \sum_{j \in N_i^\alpha} a_{ij}(q)(p_j - p_i) \\ u_i^\beta &= c_1^\beta \sum_{k \in N_i^\beta} \phi_\beta(\|\hat{q}_{i,k} - q_i\|_\sigma) \hat{\mathbf{n}}_{i,k} \\ &\quad + c_2^\beta \sum_{j \in N_i^\beta} b_{i,k}(q)(\hat{p}_{i,k} - p_i) \\ u_i^\gamma &= -c_1^\gamma \sigma_1(q_i - q_r) - c_2^\gamma (p_i - p_r) \end{aligned} \tag{59}$$

where $\sigma_1(z) = z/\sqrt{1 + \|z\|^2}$ and c_η^ν are positive constants for all $\eta = 1, 2$ and $\nu = \alpha, \beta, \gamma$. The pair (q_r, p_r) is the state of a static/dynamic γ-agent. The vectors $\mathbf{n}_{i,j}$ and $\hat{\mathbf{n}}_{i,k}$ are given by

$$\mathbf{n}_{ij} = \frac{q_j - q_i}{\sqrt{1 + \epsilon \|q_j - q_i\|^2}} \quad \hat{\mathbf{n}}_{i,k} = \frac{\hat{q}_{i,k} - q_i}{\sqrt{1 + \epsilon \|\hat{q}_{i,k} - q_i\|^2}}.$$

The only missing piece of the puzzle is the method of calculation of position and velocity of β-agents that is discussed next.

In terms of sensing requirements, we assume that every α-agent is equipped with *range sensors* that allow the agent to measure the relative position between the closest point on an obstacle and itself. Both *radars* and *laser radars* (or ladars) can be used as range sensors.

D. Calculation of Position and Velocity of β-Agents

Given an obstacle O_k and its neighboring α-agent with state (q_i, p_i), the position and velocity of a β-agent on a wall or a sphere is given by the following lemma.

Lemma 4: Let $\hat{q}_{i,k}, \hat{p}_{i,k}$ with $(i,k) \in \mathcal{V}_\alpha \times \mathcal{V}_\beta$ denote the position and velocity of a β-agent generated by an α-agent with state (q_i, p_i) on an obstacle O_k. Then, the following hold.

i) For an obstacle with a hyperplane boundary that has a unit normal $\mathbf{a}_k$ and passes through the point y_k, the position and velocity of the β-agent are determined by

$$\hat{q}_{i,k} = Pq_i + (I - P)y_k \quad \hat{p}_{i,k} = Pp_i$$

where $P = I - \mathbf{a}_k \mathbf{a}_k^T$ is a projection matrix.

ii) For a spherical obstacle with radius R_k centered at y_k, the position and velocity of the β-agent are given by

$$\hat{q}_{i,k} = \mu q_i + (1 - \mu)y_k \quad \hat{p}_{i,k} = \mu P p_i$$

where $\mu = R_k/\|q_i - y_k\|, \mathbf{a}_k = (q_i - y_k)/\|q_i - y_k\|$, and $P = I - \mathbf{a}_k \mathbf{a}_k^T$.

Proof: See the proof of [51, Lemma 3]. □

The following lemma demonstrates that the second term in u_i^β is in fact a valid damping force. This fact is used later to establish that the overall particle system is dissipative.

Lemma 5: The force $\hat{f}_d$ between α-agents and β-agents with elements $\hat{f}_i^d = \sum_{k\in N_i^\beta} b_{i,k}(p_i - \hat{p}_{i,k})$ is a valid damping force, i.e., let $K_r = (1/2)\sum_i \|p_i\|^2$ and suppose $\dot{p}_i = \hat{f}_i^d$, then $\dot{K}_r \leq 0$.

Proof: See the proof of [51, Lemma 4]. ■

E. Analysis of Flocking With Obstacle Avoidance

A natural question is whether the particle system obtained by applying Algorithm 3 is dissipative. The answer in this case is not as predictable as the case of interactions among α-agents. The reason is that in free-flocking, every α-agent reciprocates the action of its neighboring α-agents, but in constrained flocking the (α, β) proximity net is a directed graph.

Theorem 5: Consider a particle system applying Algorithm 3 [or protocol (58)]. Assume that the γ-agent is a static agent with a fixed state $(q_r, p_r) = (q_d, p_d)$. Define the energy function $H(q,p) = V(q) + T(q,p)$ with kinetic energy $T(q,p) = (1/2)\sum_{i=1}^n \|p_i\|^2$. Suppose there exists a finite time $t_0 \geq 0$ such that the average velocity of all agents satisfies the condition

$$\frac{n}{2}\langle p_c(t), p_d\rangle \leq T(q(t), p(t)) \qquad \forall t \geq t_0. \tag{60}$$

Then, the energy of the system is monotonically decreasing (i.e., $\dot{H}(q(t), p(t)) \leq 0$) along the trajectory of the collective dynamics of the mutli-species system for all $t \geq t_0$.

Proof: See the proof of [51, Th. 6]. □

The interpretation of condition (60) for a group of particles with equal velocities is interesting. In this case, $p_c = p_i$ for all i, and therefore (60) reduces to the inequality $p_c^T p_d \leq \|p_c\|^2$. Let $\theta_{c,d}$ denote the misalignment angle between vectors p_c and p_d in $\mathbb{R}^m$, i.e., $\cos(\theta_{c,d}) = \langle p_c \cdot p_d\rangle / (\|p_c\| \cdot \|p_d\|)$. Suppose $p_c, p_d \neq 0$, then the group has to be sufficiently agile, or $\|p_c\| \geq v_0 := \|p_d\|\cos(\theta_{c,d})$. Intuitively, this can be interpreted as a collective effort by the group to keep up with the desired velocity p_d. *For a γ-agent with $p_d = 0$, condition* (60) *trivially holds.*

Analysis of an equilibrium state of a group of dynamic agents that perform flocking in presence of obstacles makes less sense when the flock does not pass around all the obstacles. To be more precise, it is less interesting to analyze the stability of the equilibrium of collective dynamics of a flock while some β-agents are permanently present. This is certainly not the case for problems such as *sensor placement* and *distributed sensing* [15]. On the other hand, if one assumes that after some finite time $t_1 > 0$, no α-agent ever comes near an obstacle, the case reduces to analysis of free-flocking that has already been presented. Hence, we postpone a comprehensive analysis of the behavior of flocks in permanent presence of obstacles for mobile sensor networks to a future occasion.

F. Flocking Using a Peer-to-Peer Network

The information flow in flocking with obstacle avoidance has a natural hierarchical architecture as shown in Fig. 6(a). A γ-agent has the role of a *virtual-leader* (or commander) in charge of navigation and control of the behavior of a flock as a whole. As a result, the hierarchy in Fig. 6(a) can be referred to as a *virtual-leader/follower architecture*. The dashed line between the γ-agent and all α-agents indicates a single information exchange at $t = 0$ (otherwise, the algorithm becomes centralized). Note that a virtual-leader/follower architecture should not be confused with a leader/follower architecture in which the leader is one of the physical agents (e.g., a vehicle in a multi-vehicle system or a fish in a school).

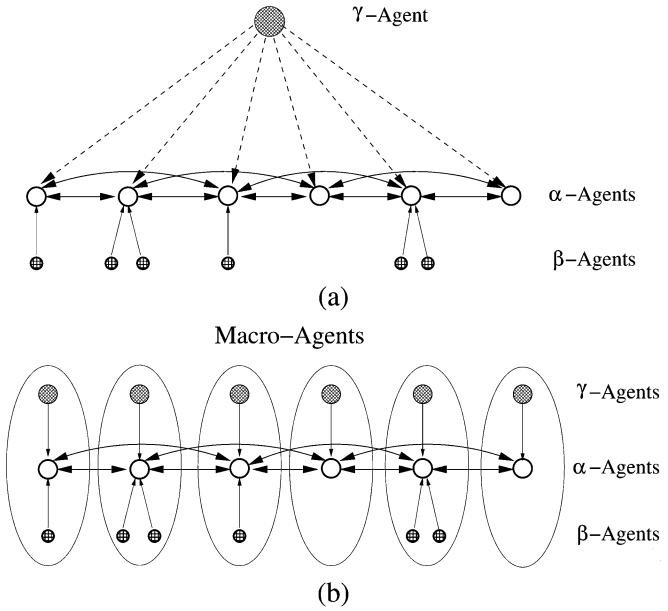

Fig. 6. In-agent and intra-agent information flow in constrained flocking. (a) Virtual-leader/follower hierarchical architecture. (b) Peer-to-peer architecture.

Since the computation required for implementation of virtual agents has to be carried out by embedded computers of a physical agent, Fig. 6(a) *does not* provide a realistic picture of the computational architecture necessary for implementation of Algorithm 3. Though, the hierarchical architecture is useful in understanding why a γ-agent plays the role of a unifying objective that brings all the α-agents together and assembles a connected network of mobile agents.

To model the information flow of Algorithm 3, we create one γ-agent corresponding to each α-agent as shown in Fig. 6(b). The new architecture is a *peer-to-peer network* that represents the interactions of a group of *macro-agents* (see Fig. 6(b)). Each macro-agent consists of an α-agent and its corresponding γ- and β-agents as illustrated in Fig. 6(b). This figure demonstrates that Algorithms 1 and 2 are special cases of Algorithm 3 and can be implemented using a peer-to-peer network.

In this network of macro-agents, two macro-agents only communicate the state of their public components (i.e., α-agents). Under the assumption that the initial state and dynamics of all γ-agents are equal, the virtual-leader/follower and peer-to-peer architectures become equivalent representations of a multi-species particle system.

The biological implication of feasibility of performing tracking/migration for groups of dynamic agents using a peer-to-peer network is that *"flocks need no leaders"*. This mathematically confirms a fact that has been known to animal behavior scientists for years [1].

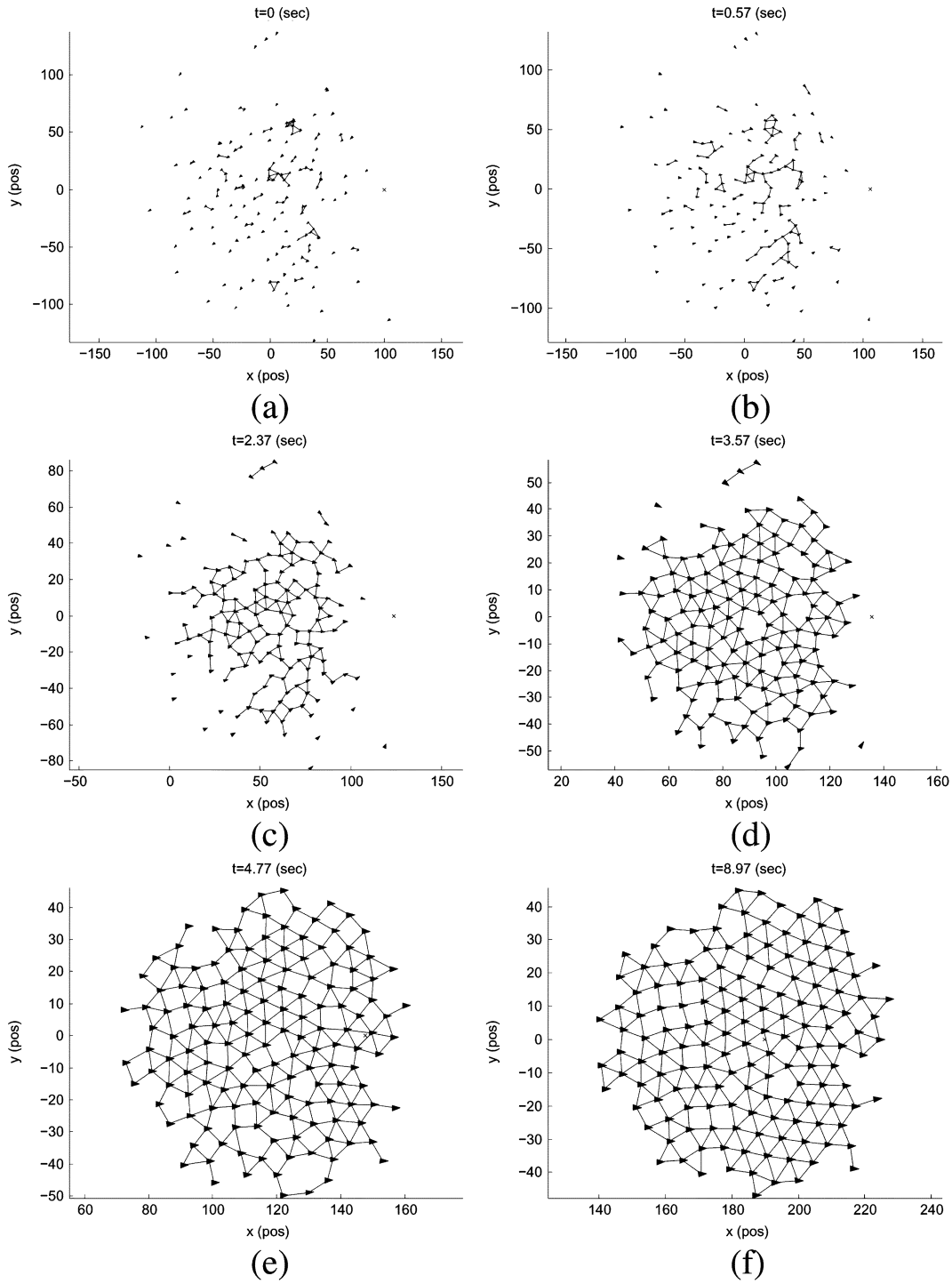

Fig. 7. 2-D flocking for $n = 100$ agents applying Algorithm 2.

VIII. Simulation Results

In this section, we present several simulation results of 2-D and 3-D flocking. The following parameters remain fixed throughout all simulations: $d = 7, r = 1.2d$ (or $\kappa = 1.2$), $d' = 0.6d, r' = 1.2d', \epsilon = 0.1$ (for σ-norm), $a = b = 5$ for $\phi(z)$, $h = 0.2$ for the bump function of $\phi_\alpha(z)$, $h = 0.9$ for the bump function of $\phi_\beta(z)$, and the step-size in all simulations ranges between 0.01–0.03 s (equivalent to an update frequency of 33–100 Hz). The parameters of the flocking algorithms and the types of the initial states are specified separately for each experiment. The set of l spherical obstacles are specified with an $(m+1) \times l$ matrix M_s where each column of M_s is the vector $\text{col}(y_k, R_k) \in \mathbb{R}^{m+1}$.

In all simulation results, the heading angle (or attitude) of each α-agent specifies the direction of the velocity of that agent. In addition, the position of a dynamic γ-agent is marked with a $\times$ sign.

A. 2-D Flocking in Free-Space ($n = 150$)

Fig. 7 shows consecutive snapshots of the proximity structure during 2-D flocking for 150 agents in free-space using

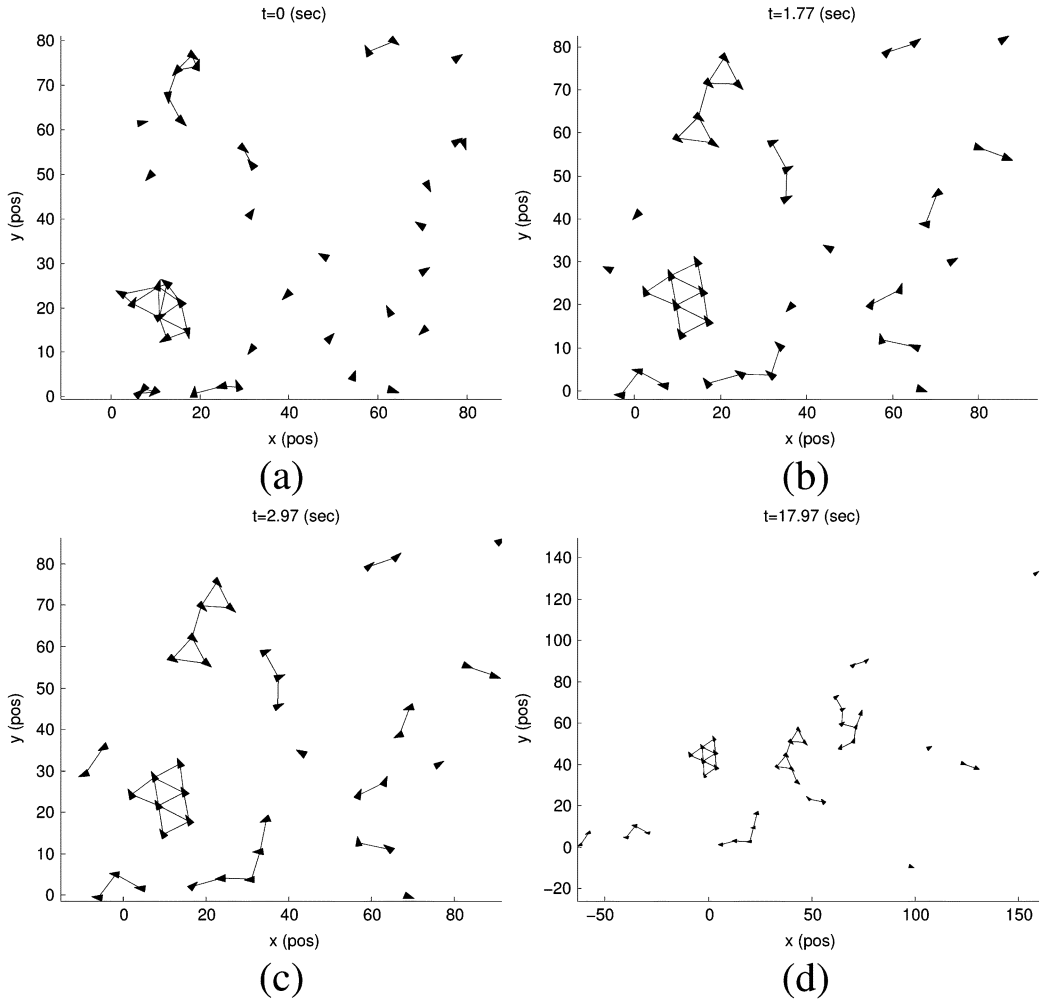

Fig. 8. Fragmentation for 40 agents applying Algorithm 1.

Algorithm 2. The initial positions are chosen randomly from a Gaussian distribution with variance of 2500. The initial velocity coordinates are uniformly chosen at random from the box $[-2,-1]^2$. A flock is formed in Fig. 7(d) and maintained thereafter. A dynamic γ-agent is used for this example. The number of edges of the proximity net $G(q(t))$ increases by time and has a tendency to render the network connected. The set of initial positions are chosen uniformly at random so that the initial proximity net $G(q(0))$ is highly disconnected (i.e., has too many components). This makes the task of flocking more challenging. The planarity of the proximity structures in Figs. 7(c) through (f) is very clear. Numerical measurements indicate that the final conformation is a low-energy quasi α-lattice that induces a connected proximity net [see Fig. 12(a)]. These observations are in close agreement with our theoretical predictions in Section V.

B. 2-D Fragmentation in Free-Space $(n = 40)$

Fig. 8 demonstrates the fragmentation phenomenon for $n = 40$ agents applying Algorithm 1. It is not surprising that with a random set of initial states, flocking behavior is not created. In Fig. 8(f), one can identify nine distinct small components of the proximity net (each contains at list two agents) and three individual agents.

In Algorithm 1 (or (α, α) protocol), no γ-agent exists due to lack of existence of a group objective. This simulation result is another evidence that demonstrates creation of flocking motion is rather nontrivial because the idea of using a gradient-based control law plus a velocity matching term does not necessarily work!

Fragmentation is a generic form of collective behavior of agents applying Algorithm 1. This behavior is insensitive to the type of probability distribution of the initial position of the agents. Apparently, for the case of a highly dense initial proximity net with small initial velocity mismatch, one might expect that the group of agents form a quasi-flock.

In Figs. 8(d)–(f), it can be observed that two agents which belong to two different components of the proximity net, move further apart from each other as time goes by. Again, this is a generic property of fragmentation. Fragmentation phenomenon can be viewed as lack of cohesion in a group of particles [see Fig. 12(b)].

C. 3-D Flocking in Free-Space: Automated Rendezvous

Fig. 9 shows the consecutive snapshots of 3-D flocking for a group of $n = 50$ agents using Algorithm 2. Each agent represents a UAV moving in $\mathbb{R}^3$. The initial state of the agents is chosen at random with a Gaussian distributed. The attitude

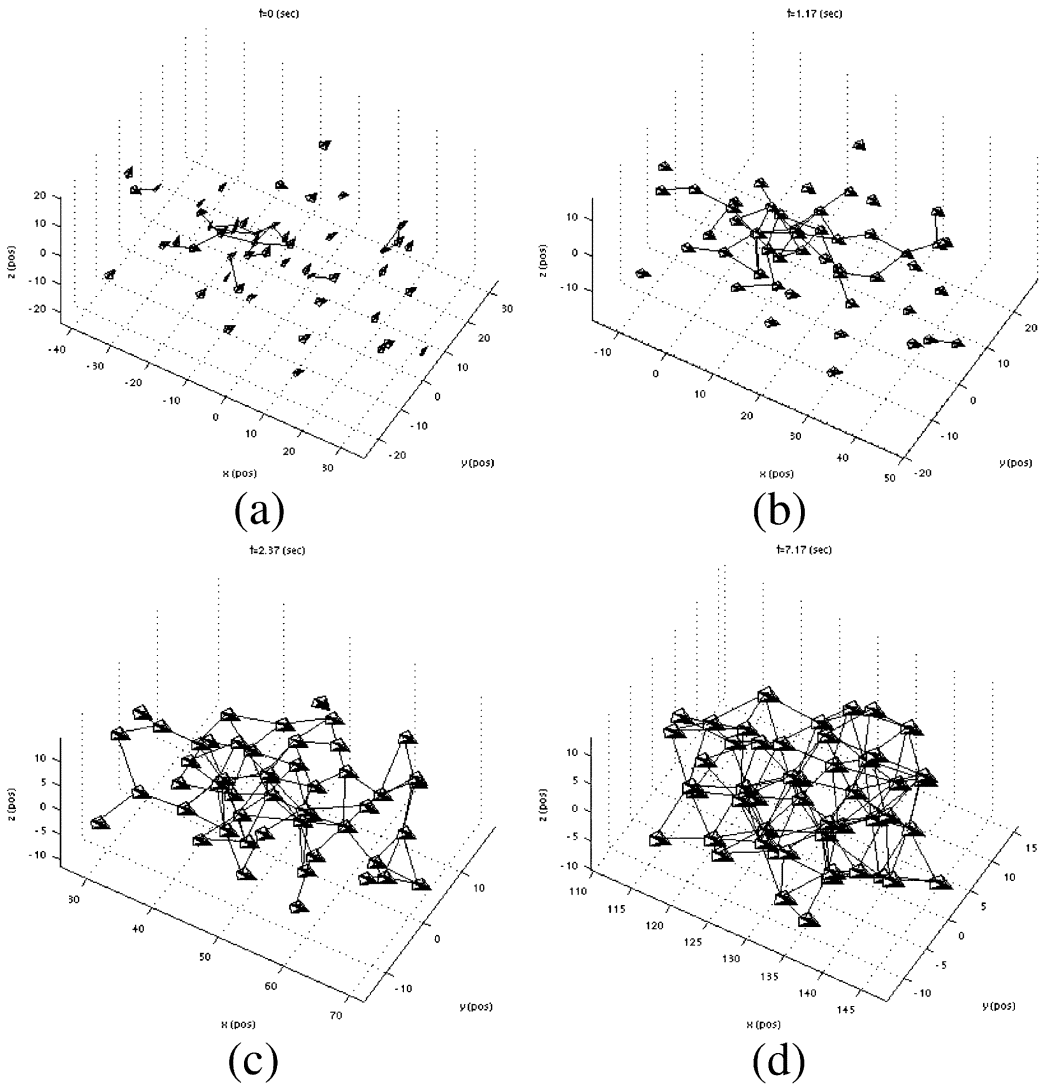

Fig. 9. Snapshots of 3-D flocking/automated rendezvous using Algorithm 2 for $n = 50$ UAVs.

of each UAV is a rotation matrix $R_i \in SO(3)$ with columns r_1, r_2, r_3. We use the following steps to determine R_i from velocity $p_i \neq 0$: i) set $r_1 = p_i/\|p_i\|$ and let $e_3 = (0,0,1)^T$, ii) set $r_2 = e_3 \times r_1$, and iii) set $r_3 = r_1 \times r_2$ ($\times$ denotes the cross-product in $\mathbb{R}^3$). For $p_i = 0$, define $R_i = I_3$. Based on this experiment, flocking can be used as a means of *automated rendezvous* (or gathering) for a medium to large number of autonomous agents. It is apparent that after some finite time, the agents self-assemble a flock and maintain its connectivity thereafter. The formal proof of this statement requires the proof of Conjecture 1 in Section V.

D. Split/Rejoin Maneuver: Low-Altitude Flight of UAVs and Predator Evasion

Consider a group of agents that intend to move/migrate from point A to B. Here, A and B are the positions of the CM of the group at the group's source and destination. Whenever there are multiple obstacles along the straight line connecting A to B, the agents cannot pass through the obstacles. As a result, they might split in two or multiple smaller groups. This maneuver is useful for missions that require low-altitude flight of UAVs or moving in urban environments. In schools of fish, the split/rejoin maneuver is used as a predator evasion tactic [3].

The objective in performing a *split/rejoin maneuver* is to gather various groups that have initially split due to the presence of obstacles or adversarial agents. The split/rejoin maneuver is demonstrated in Fig. 10 for a group of $n = 150$ agents in presence of $l = 6$ obstacles. Based on Fig. 10, it is clear that the proximity net of dynamic agents during flocking undergoes frequent changes. In other words, flocking involves stability analysis for a network of dynamic systems with switching topology (e.g., [21]).

The initial position of the agents are chosen uniformly at random from the box $[-40, 80]^2$. The initial velocities are set to zero. The group objective is specified by a static γ-agent with $q_d = (200, 30)^T$ and $p_d = (5, 0)^T$. Moreover, $c_1^\alpha < c_1^\gamma < c_1^\beta$ and $c_2^\gamma = 2\sqrt{c_1^\gamma}$ for all species. The matrix of obstacles is

$$M_s = \begin{bmatrix} 100 & 110 & 120 & 130 & 150 & 160 \\ 20 & 60 & 40 & -20 & 40 & 0 \\ 10 & 4 & 2 & 5 & 5 & 3 \end{bmatrix}.$$

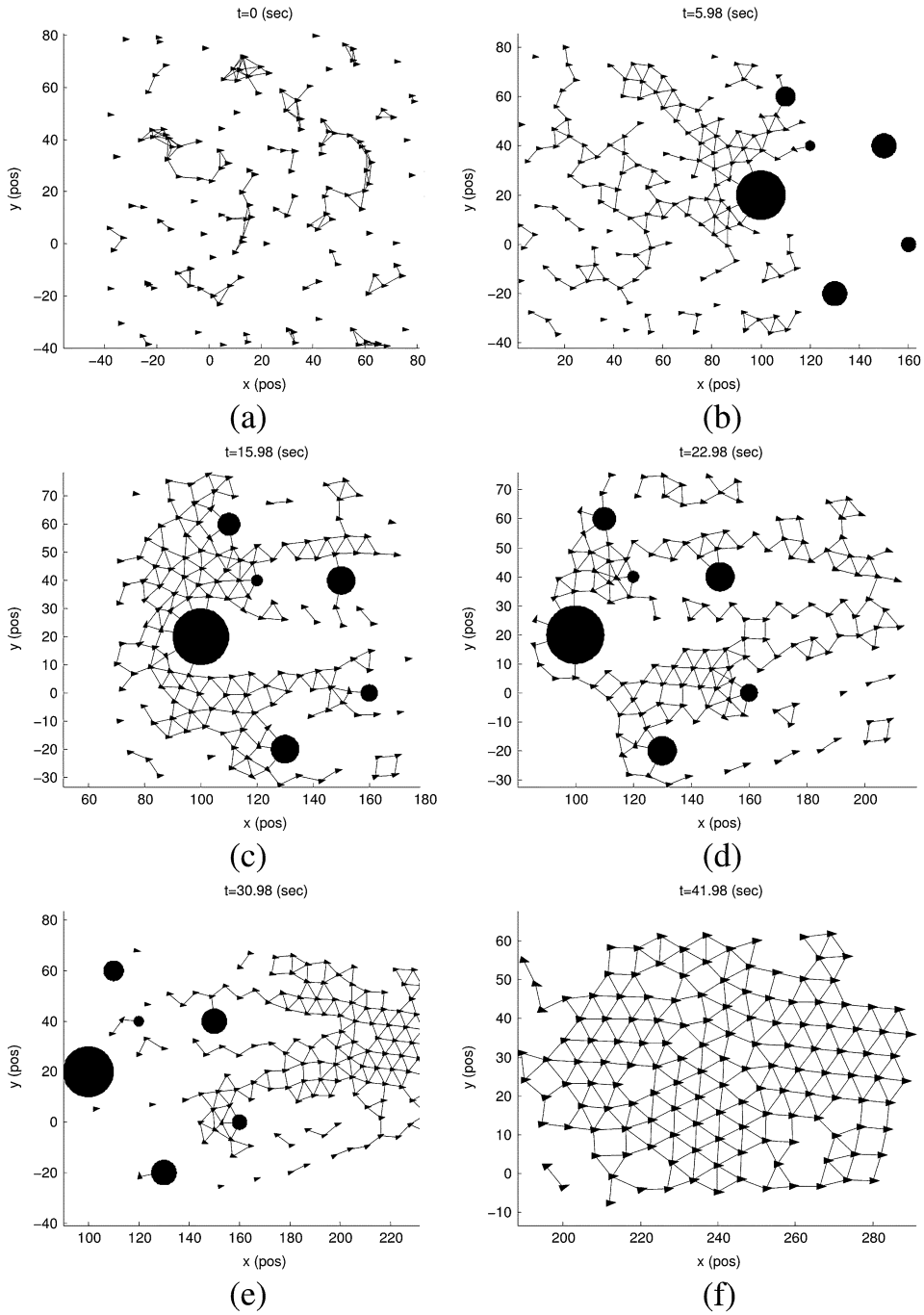

Fig. 10. Split/rejoin maneuver for $n = 150$ agents.

Based on Fig. 10, after all agents pass the obstacles on their way, the group forms a large flock. It was numerically verified that no agent ever entered any of the six obstacles for the complete trajectory of the particles.

E. Squeezing Maneuver: Moving Through Narrow Spaces

The *squeezing maneuver* is the result of flocking in presence of obstacles that are relatively close to each other. This a special case of escape panic phenomenon. By "relatively close," we mean that the narrow pathway between the obstacles is about $2r$ to $3r$ wide. Fig. 11 illustrates the task of squeezing maneuver for $n = 150$ agents. The initial positions of the agents are $n = 150$ random points that are uniformly distributed in the box $[0, 120]^2$. The initial velocity of all agents is set to zero. For this case, the group objective is specified by a static γ-agent with $q_d = (230, 60)^T$ and $p_d = (6, 0)^T$. In addition, $c_1^\alpha < c_1^\gamma < c_1^\beta$ and $c_2^\nu = 2\sqrt{c_1^\nu}$ for $\nu = \alpha, \beta, \gamma$. The matrix of obstacles is given by

$$M_s = \begin{bmatrix} 150 & 150 \\ 30 & 100 \\ 25 & 25 \end{bmatrix}.$$

According to Fig. 11, one can observe that the agents avoid collision with both obstacles as moving forward. This has been nu-

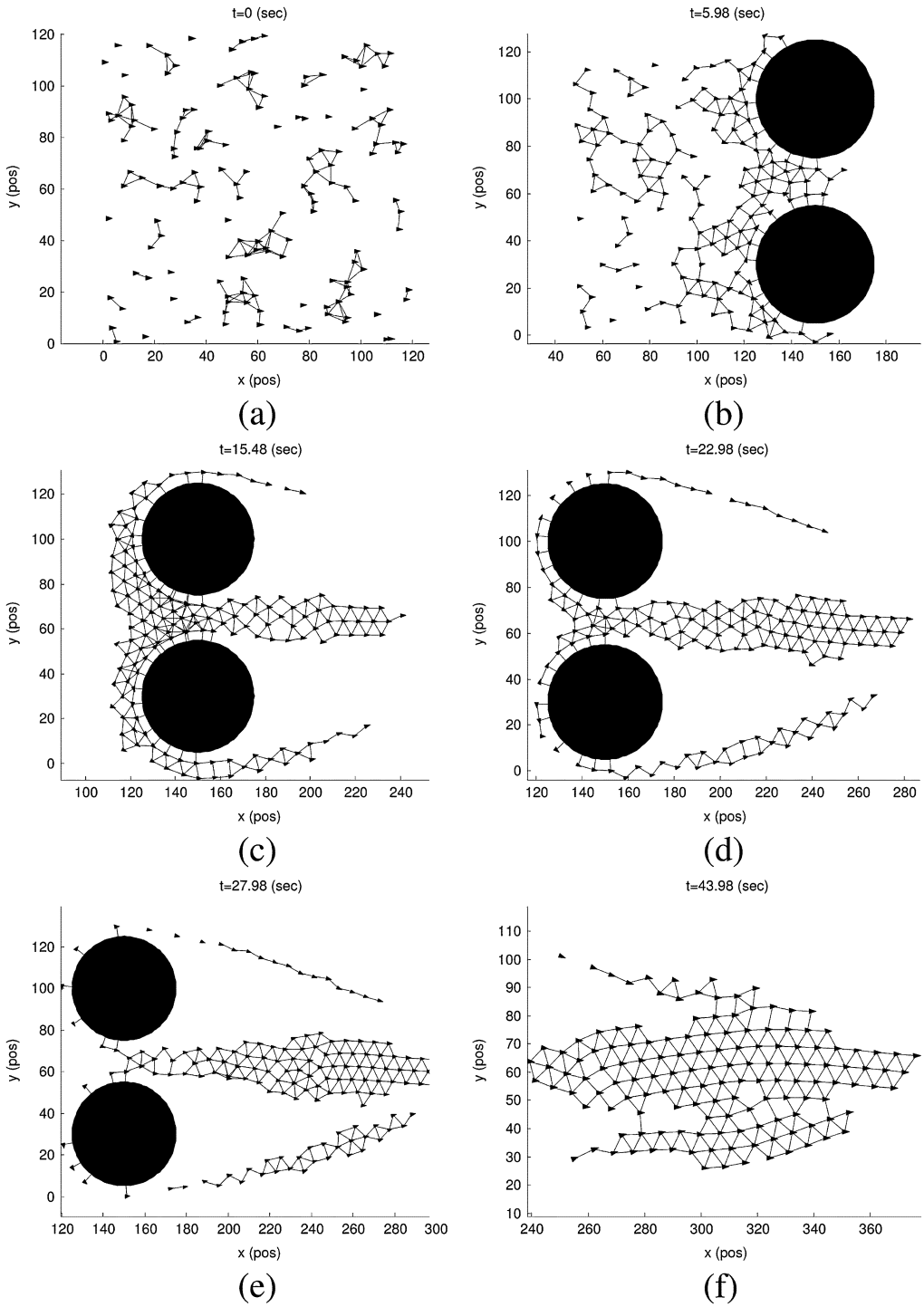

Fig. 11. Squeezing maneuver for $n = 150$ agents.

merically verified for the entire trajectory of the particles. Since the desired group velocity is nonzero, the group does not stop near q_d and moves along the specified desired group velocity p_d. After passing both obstacles, the agents form a large flock as shown in Fig. 11(f).

IX. What Constitutes Flocking?

In [52], Partridge provides a brief survey of various definitions of "schooling in fish" by animal behavior scientists that spans half a century from 1927 to 1981. The length of this period is a clear indication of the difficulty of the task in hand. To give an objective definition of flocking, we determine a quantitative measure of flocking that is independent of collective dynamics of the agents. In the sense that it does not depend on a specific method used for generation of trajectories of particles, i.e., the measure is *universal*. In the following, we define a special form of flocking called α-flocking.

Definition 4 (α-Flocking): Let $z : t \mapsto \mathrm{col}(q(t), p(t))$ be the state trajectory of a system of n dynamic agents (or particles).

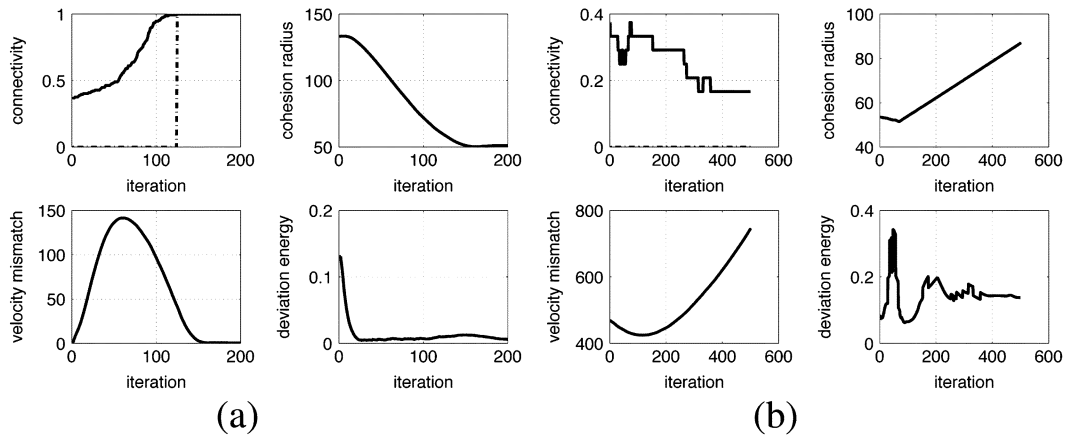

Fig. 12. $C, R, \bar{E}, \bar{K}$ curves (in clock-wise order). (a) Flocking. (b) Regular fragmentation.

We say a group of agents perform α-*flocking* over the time interval $[t_0, t_f]$ if there exists relatively small numbers $\epsilon_0, \epsilon_1, \epsilon_2 > 0$ and a distance $d > 0$ such that the trajectory $z(t)$ satisfies all the following conditions for all $t \in [t_0, t_f]$ with an interaction range $r = (1 + \epsilon_0)d$:

i) the group remains a quasi-flock;
ii) the group remains cohesive;
iii) the deviation energy remains small $(E(q(t)) \leq \epsilon_1 d^2)$;
iv) the velocity mismatch remains small $(K(v(t)) \leq \epsilon_2 n)$.

A more strict form of flocking, or *strict* α-*flocking*, can be defined by replacing the above four conditions with the following three properties.

a) The group remains a flock (i.e., the proximity net $G(q(t))$ remains connected).
b) The deviation energy remains small $(E(q(t)) \leq \epsilon_1 d^2)$.
c) The velocity mismatch remains small $(K(v(t)) \leq \epsilon_2 n)$.

One can use conditions a) and b) to establish that the group remains cohesive over the interval $[t_0, t_f]$. Definition 4 has the same role for flocking in particle systems that Lyapunov stability has for nonlinear dynamical systems. It is worthwhile mentioning that "regular fragmentation" violates conditions i), ii), and iv) of Definition 4, "irregular fragmentation" violates all four conditions of α-flocking, and "irregular collapse" severely violates condition iii). Therefore, irregular/regular fragmentation and irregular collapse do not constitute α-flocking as mentioned in Section I. Furthermore, "regular collapse" is an acceptable form of α-flocking for when a comfortable/safe inter-agent distance d is replaced by an uncomfortable distance $d' \ll d$. Surprisingly, regular collapse phenomenon can be found in nature as a defense mechanism used by schools of fish. Recent results on collapse phenomenon for self-driven particle systems can be found in D'Orsogna *et al.* [53].

Formation flight (e.g., for birds) can be viewed as the *most strict form of* α-*flocking* with $\epsilon_1 = \epsilon_2 = 0$ and a fixed topology $G(q(t)) = G(t_0), \forall t \in [t_0, t_f]$. This is consistent with the prediction of Theorem 2 (part ii) that asymptotically the topology of a flock of α-agents evolves to a fixed graph $G^* = G(x^*_\lambda)$.

The main feature of Definition 4 is that α-flocking can be numerically verified for the trajectories of a system of particles regardless of the method of trajectory generation. Meaning that the definition of α-flocking is *universal* (or algorithm-independent). This is analogous to universality of the definition of "Lyapunov stability" for nonlinear systems (Lyapunov stability is a property of the solutions of a nonlinear system and not its vector field). The challenge is to search for parameters $\epsilon_0, \epsilon_1, \epsilon_2, d$. This verification process is discussed next.

A. Verification of α-Flocking

To verify whether a group of particles perform α-flocking, we need to calculate four quantities along the trajectory of the particles. These quantities are defined in the following.

i) *Relative Connectivity:* Since the rank of Laplacian of a connected graph of order n is at most $(n-1)$, we define the *relative connectivity* of the group at time t as $C(t) = (1/n - 1)\text{rank}(L(q(t))) \in [0, 1]$, where $L(q)$ is the adjacency matrix of a graph with 0-1 adjacency elements corresponding to the set of edges of the proximity net $G(q)$.
ii) *Cohesion Radius:* We define the *cohesion radius* of a group of agents at time t as $R(t) = \max_{i \in \mathcal{V}} \|q_i(t) - q_c(t)\|$. A cohesive group has a finite cohesion radius.
iii) *Normalized Deviation Energy:* $\tilde{E}(q) = E(q)/d^2$.
iv) *Normalized Velocity Mismatch:* $\tilde{K}(v) = K(v)/n$.

To clarify the use of these quantities, consider the trajectory of $n = 150$ particles applying Algorithm 2. The curves $C, R, \tilde{E}, \tilde{K}$ for this trajectory are plotted in Fig. 12(a) over the first 200 iterations. (The step-size is $T = 0.03$ (s) and $t = kT$ where k is the iteration number.) At iteration $k_c > 100$, a phase transition occurs and the proximity net $G(q(t))$ becomes connected. Clearly, the network topology remains connected for all future iterations $k > k_c$. The point $k = k_c$ is shown by a dished line. The effect of this phase transition is clear in the (normalized) velocity mismatch curve for $k > k_c$. In this case, the cohesion radius is monotonically decreasing. It is also clear that the (normalized) energy deviation remains relatively small after $k = 150$ iterations. Based on the simulation data, we conclude that α-flocking is achieved after the 150th iteration with parameters $\epsilon_0 = 0.2, \epsilon_1 = 0.005, \epsilon_2 = 0.3$.

In contrast, Fig. 12(b) shows the four curves obtained from the trajectory of particles during fragmentation for $n = 50$ agents. Here are some observations: 1) the cohesion radius is monotonically increasing after a brief period, 2) the proximity net never becomes connected and has too many components, 3) the velocity mismatch never reduces below a large constant and

is increasing after a brief period, and 4) the deviation energy remains relatively low. All these facts point out to the occurrence of regular fragmentation phenomenon.

X. Conclusion

This paper provides a theoretical framework for design and analysis of distributed flocking algorithms for mutli-agent networked systems. The cases of free-flocking and flocking with obstacle avoidance were both addressed. α-lattices as geometric models of flocks play a crucial role in both construction of collective potential functions for flocking as well as analysis of flocking behavior.

Three distributed flocking algorithms were introduced that lead to self-organizing flocking behavior. We demonstrated that Algorithm 1 is responsible for creation of spatial-order in flocks. This algorithm generically leads to regular fragmentation and embodies all three rules of Reynolds in a single equation. Algorithms 2 and 3 both evolved from Algorithm 1 by adding appropriate terms that account for group objective and obstacle avoidance, respectively. We demonstrated that generically Algorithm 2 leads to flocking, whereas Algorithm 1 leads to fragmentation. The concepts of "flocks" and "flocking" were formally defined and numerically verified. Both split/rejoin maneuver and squeezing maneuver were successfully performed using Algorithm 3 for 150 agents.

Acknowledgment

The author would like to thank R. M. Murray, J. Marsden, J. S. Shamma, E. Frazzoli, A. Bertozzi, and E. Feron for their comments and encouragements. He would also like to thank the anonymous reviewers and the Associate Editor for their valuable comments. Observing flocking, schooling, and swarming behavior in nature has truly inspired this work.

References

[1] E. Shaw, "Fish in schools," *Natural History*, vol. 84, no. 8, pp. 40–45, 1975.

[2] B. L. Partridge, "The chorus-line hypothesis of maneuver in avian flocks," *Nature*, vol. 309, pp. 344–345, 1984.

[3] ——, "The structure and function of fish schools," *Sci. Amer.*, vol. 246, no. 6, pp. 114–123, 1982.

[4] A. Okubo, "Dynamical aspects of animal grouping: Swarms, schools, flocks. and herds," *Adv. Biophys.*, vol. 22, pp. 1–94, 1986.

[5] C. W. Reynolds, "Flocks, herds, and schools: A distributed behavioral model," in *Comput. Graph. (ACM SIGGRAPH'87 Conf. Proc.)*, vol. 21, Jul. 1987, pp. 25–34.

[6] T. Vicsek, A. Czirok, E. Ben-Jacob, I. Cohen, and O. Shochet, "Novel type of phase transition in a system of self-deriven particles," *Phys. Rev. Lett.*, vol. 75, no. 6, pp. 1226–1229, 1995.

[7] J. Toner and Y. Tu, "Flocks, herds, and schools: A quantitative theory of flocking," *Phys. Rev. E*, vol. 58, no. 4, pp. 4828–4858, Oct. 1998.

[8] N. Shimoyama, K. Sugawara, T. Mizuguchi, Y. Hayakawa, and M. Sano, "Collective motion in a system of motile elements," *Phys. Rev. Lett.*, vol. 76, no. 20, pp. 3870–3873, 1996.

[9] A. Mogilner and L. Edelstein-Keshet, "A nonlocal model for a swarm," *J. Math. Biol.*, vol. 38, pp. 534–570, 1999.

[10] D. Helbing, I. Farkas, and T. Vicsek, "Simulating dynamical features of escape panic," *Nature*, vol. 407, pp. 487–490, 2000.

[11] T. Vicsek, "A question of scale," *Nature*, vol. 411, pp. 421–421, May 2001.

[12] J. K. Parrish, S. V. Viscido, and D. Grunbaum, "Self-organized fish schools: An examination of emergent properties," *Biol. Bull.*, vol. 202, pp. 296–305, 2002.

[13] D. Estrin, R. Govindan, J. Heidemann, and S. Kumar, "Next century challenges: Scalable coordination in sensor networks," *Proc. Mobile Comput. Network.*, pp. 263–270, 1999.

[14] I. Akyildiz, W. Su, Y. Sankarasubramniam, and E. Cayirci, "A survey on sensor networks," *IEEE Commun. Mag.*, no. 8, pp. 102–114, Aug. 2002.

[15] J. Cortes and F. Bullo, "Coordination and geometric optimization via distributed dynamical systems," *SIAM J. Control Optim.*, no. 5, pp. 1543–1574, May 2005.

[16] R. Olfati-Saber, "Distributed Kalman filter with embedded consensus filters," in *Proc. 44th IEEE Conf. Decision and Control and Eur. Control Conf.*, Dec. 2005, pp. 8179–8184.

[17] H. Levine, W.-J. Rappel, and I. Cohen, "Self-organization in systems of self-propelled particles," *Phys. Rev. E*, vol. 63, p. 017 101, 2001.

[18] A. Mogilner and L. Edelstein-Keshet, "Spatio-temporal order in populations of self-aligning objects: Formation of oriented patches," *Physica D*, vol. 89, pp. 346–367, 1996.

[19] C. M. Topaz and A. L. Bertozzi, "Swarming patterns in a two-dimensional kinematic model for biological groups," *SIAM J. Appl. Math.*, May 2004.

[20] R. O. Saber and R. M. Murray, "Consensus protocols for networks of dynamic agents," in *Proc. Amer. Control Conf.*, vol. 2, Jun. 2003, pp. 951–956.

[21] R. Olfati-Saber and R. M. Murray, "Consensus problems in networks of agents with switching topology and time-delays," *IEEE Trans. Autom. Control*, vol. 49, no. 9, pp. 1520–1533, Sep. 2004.

[22] A. Jadbabaie, J. Lin, and A. S. Morse, "Coordination of groups of mobile agents using nearest neighbor rules," *IEEE Trans. Autom. Control*, vol. 48, no. 6, pp. 988–1001, Jun. 2003.

[23] L. Moreau, "Stability of multiagent systems with time-dependent communication links," *IEEE Trans. Autom. Control*, vol. 50, no. 2, pp. 169–182, Feb. 2005.

[24] W. Ren and R. W. Beard, "Consensus seeking in multiagent systems under dynamically changing interaction topologies," *IEEE Trans. Autom. Control*, vol. 50, no. 5, pp. 655–661, May 2005.

[25] R. Olfati-Saber, A. Fax, and R. M. Murray, "Consensus and cooperation in multi-agent networked systems," *Proc. IEEE*, http://engineering.dartmouth.edu/~olfati/papers/olfati-saber-piece.pdf, 2006, submitted for publication.

[26] Y. Liu, K. M. Passino, and M. M. Polycarpou, "Stability analysis of M-dimensional asynchronous swarms with a fixed communication topology," *IEEE Trans. Autom. Control*, vol. 48, no. 1, pp. 76–95, Jan. 2003.

[27] E. W. Justh and P. S. Krishnaprasad, "A simple control law for UAV formation flying," Inst. Syst. Res., Univ. Maryland, College Park, MD, Tech. Rep. 2002-38, 2002.

[28] V. Gazi and K. M. Passino, "Stability analysis of swarms," *IEEE Trans. Autom. Control*, vol. 48, no. 4, pp. 692–697, Apr. 2003.

[29] H. G. Tanner, A. Jadbabaie, and G. J. Pappas, "Stable flocking of mobile agents Part II: Dynamic topology," in *Proc. 42nd IEEE Conf. Decision and Control*, Dec. 2003, pp. 2016–2021.

[30] A. Fax and R. M. Murray, "Information flow and cooperative control of vehicle formations," *IEEE Trans. Autom. Control*, vol. 49, no. 9, pp. 1465–1476, Sep. 2004.

[31] M. Mesbahi, "State-dependent graphs," in *Proc. 42nd IEEE Conf. Decision and Control*, vol. 3, Dec. 2003, pp. 3058–3063.

[32] ——, "On state-dependent dynamic graphs and their controllability properties," *IEEE Trans. Autom. Control*, vol. 50, no. 3, pp. 387–392, Mar. 2005.

[33] J. Cortes, S. Martinez, T. Karatas, and F. Bullo, "Coverage control for mobile sensing networks," *IEEE Trans. Robot. Automat.*, vol. 20, no. 2, pp. 243–255, Apr. 2004.

[34] G. Ribichini and E. Frazzoli, "Efficient coordination of multiple-aircraft systems," in *Proc. 42nd IEEE Conf. Decision and Control*, vol. 1, Dec. 2003, pp. 1035–1040.

[35] N. E. Leonard and E. Fiorelli, "Virtual leaders, artificial potentials, and coordinated control of groups," in *Proc. 40th IEEE Conf. Decision and Control*, 2001, pp. 2968–2973.

[36] R. Olfati-Saber and R. M. Murray, "Distibuted cooperative control of multiple vehicle formations using structural potential functions," presented at the Proc. 15th IFAC World Congr., Barcelona, Spain, Jun. 2002.

[37] P. Ögren, E. Fiorelli, and N. E. Leonard, "Cooperative control of mobile sensor networks: Adaptive gradient climbing in a distributed environment," *IEEE Trans. Autom. Control*, vol. 49, no. 8, pp. 1292–1302, Apr. 2005.

[38] O. Khatib, "Real-time obstacle avoidance for manipulators and mobile robots," *Int. J. Robot. Res.*, vol. 5, no. 1, pp. 90–98, 1986.

[39] E. Rimon and D. E. Koditschek, "Exact robot navigation using artificial potential functions," *IEEE Trans. Robot. Automat.*, vol. 8, no. 5, pp. 501–518, Oct. 1992.
[40] S. H. Strogatz, "Exploring complex networks," *Nature*, vol. 410, pp. 268–276, 2001.
[41] R. Olfati-Saber, "Ultrafast consensus in small-world networks," in *Proc. Amer. Control Conf.*, Jun. 2005, pp. 2371–2378.
[42] D. E. Chang, S. Shadden, J. Marsden, and R. Olfati-Saber, "Collision avoidance for multiple agent systems," in *Proc. 42nd IEEE Conf. Decision and Control*, vol. 1, Dec. 2003, pp. 539–543.
[43] R. Olfati-Saber, "Flocking with obstacle avoidance," California Inst. Technol., Control Dyna. Syst., Pasadena, CA, Tech. Rep. 2003-006, Feb. 2003.
[44] R. O. Saber and R. M. Murray, "Flocking with obstacle avoidance: Cooperation with limited communication in mobile networks," in *Proc. 42nd IEEE Conf. Decision and Control*, vol. 2, Dec. 2003, pp. 2022–2028.
[45] B. Bollobás, *Modern Graph Theory, Vol. 184 of Graduate Texts in Mathematics*. New York: Springer-Verlag, 1998.
[46] R. Diestel, *Graph Theory, Vol. 173 of Graduate Texts in Mathematics*. New York: Springer-Verlag, 2000.
[47] R. A. Horn and C. R. Johnson, *Matrix Analysis*. Cambridge, U.K.: Cambridge Univ. Press, 1987.
[48] C. Godsil and G. Royle, *Algebraic Graph Theory, Vol. 207 of Graduate Texts in Mathematics*. New York: Springer-Verlag, 2001.
[49] E. Klavins, "Communication complexity of multi-robot systems," in *Algorithmic Foundations of Robotics V*. ser. Springer Tracts in Advanced Robotics, J.-D. Boissonnats, J. Burdik, K. Goldberg, and S. Huchinson, Eds. Budapest, Hungary: Springer, Dec. 2003, vol. 7, pp. 275–292.
[50] M. Fiedler, "Algebraic connectivity of graphs," *Czech. Math. J.*, vol. 23, no. 98, pp. 298–305, 1973.
[51] R. Olfati-Saber, "Flocking for multi-agent dynamic systems: Algorithms and theory," California Inst. Technol., Control Dyna. Syst., Pasadena, CA, Tech. Rep. 2004-005, http://caltechcdstr.library.caltech.edu/43/, Jun. 2004.
[52] B. L. Partridge, "Rigid definitions of schooling behavior are inadequate," *Animal Behavior*, vol. 30, pp. 298–299, Feb. 1982.
[53] M. R. D'Orsogna, Y.-L. Chuang, A. L. Bertozzi, and L. Chayes, "Self-propelled particles with soft-core interactions: Patterns, stability, and collapse," *Phys. Rev. Lett.*, vol. 96, Mar. 2006, to be published.

Reza Olfati-Saber (S'97–M'01) received the S.M. and Ph.D. degrees in electrical engineering and computer science from Massachusetts Institute of Technology, Cambridge, in 1997 and 2001, respectively.

He has been an Assistant Professor at the Thayer School of Engineering at Dartmouth College, Hanover, NH, since 2005. Prior to joining Dartmouth, he was a Postdoctoral Scholar at California Institute of Technology, Pasadena (2001-2004) and a Visiting Scientist at the University of California, Los Angeles (2004-2005). His research interests include distributed control theory, multi-agent systems, sensor networks, information fusion, distributed Kalman filtering, swarms, self-organizing networked systems, probabilistic learning and inference, social networks, small-worlds, consensus theory, and evolutionary dynamics of language, behavior, and culture. He is a member of the Sigma Xi scientific society.